P-wave superfluid in neutron star matter at low and high densities
-Perspective from cold atomic physics-

Low density: HT, H. Funaki, Y. Sekino, N. Yasutake, and M. Matsuo, Phys. Rev. C **108**, L052802 (2023).

High density: Y. Guo, HT, T. Hatsuda, and H. Liang, Phys. Rev. A **108**, 023304 (2023).

Collaborators

- **Low density**: HT, H. Funaki, Y. Sekino, N. Yasutake, and M. Matsuo, Phys. Rev. C **108**, L052802 (2023).

H. Funaki
(UCAS)

Y. Sekino
(RIKEN)

N. Yasutake
(Chiba Tech.)

M. Matsuo
(UCAS)

- **High density**: Y. Guo, HT, T. Hatsuda, and H. Liang, Phys. Rev. A **108**, 023304 (2023).

Y. Guo
(U. Tokyo)

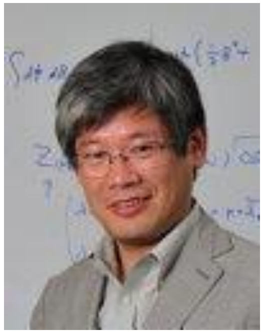

T. Hatsuda
(RIKEN)

H. Liang
(U. Tokyo)

Outline

- Brief introduction of neutron superfluid
- ${}^3P_0$ neutron superfluid at low density
- Fate of *P*-wave pairing at high density
- Summary

Outline

- Brief introduction of neutron superfluid
- $^3P_0$ neutron superfluid at low density
- Fate of P-wave pairing at high density
- Summary

Endeavor in neutron star physics

- Only system which consists of extremely dense nuclear or quark matter in nature

Structure of Neutron Star

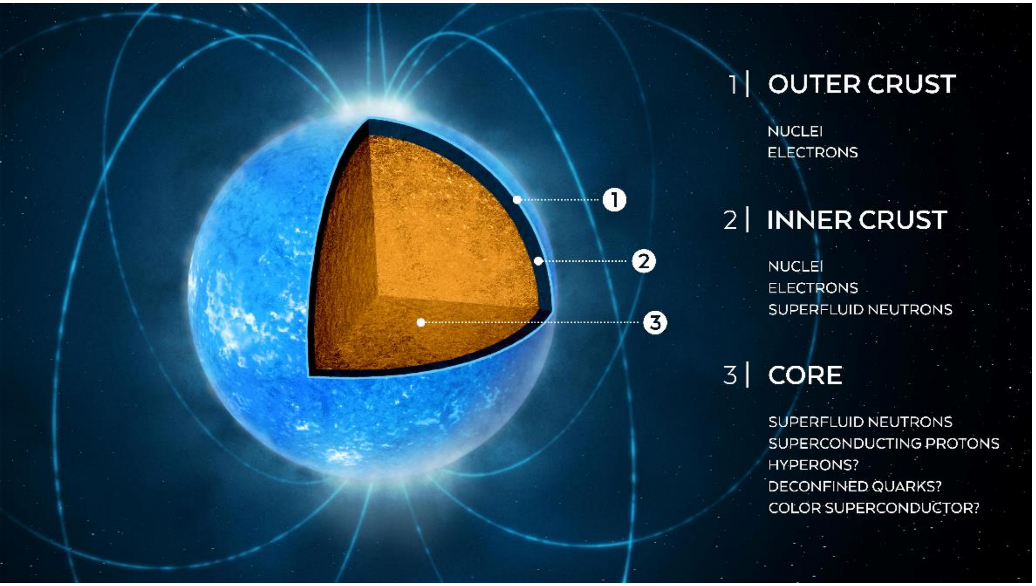

A. L. Watts, *et al.*, RMP **88**, 021001 (2016).

Cooling Curve

D. Page, Fifty Years of Nuclear BCS 324-447 (2013).

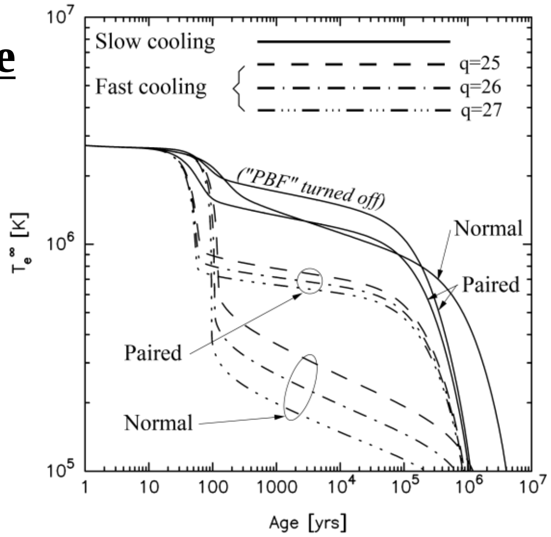

Pulsar Glitch

J. R. Fuentes, *et al.*, A&A 608, A131 (2017)

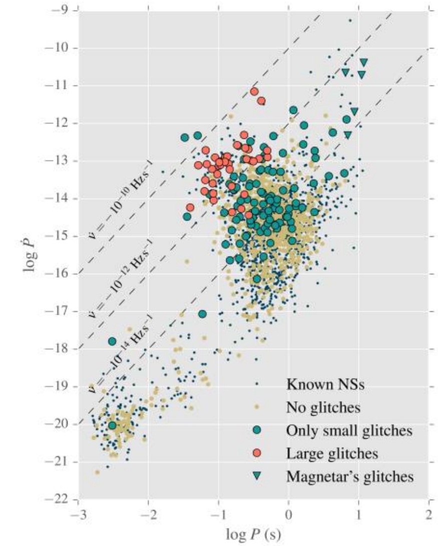

Various observations and rich physics

➡ Existence of nucleon superfluidity

Nucleon-nucleon scattering phase shift and pairing gaps

Phase shift of *NN* scattering

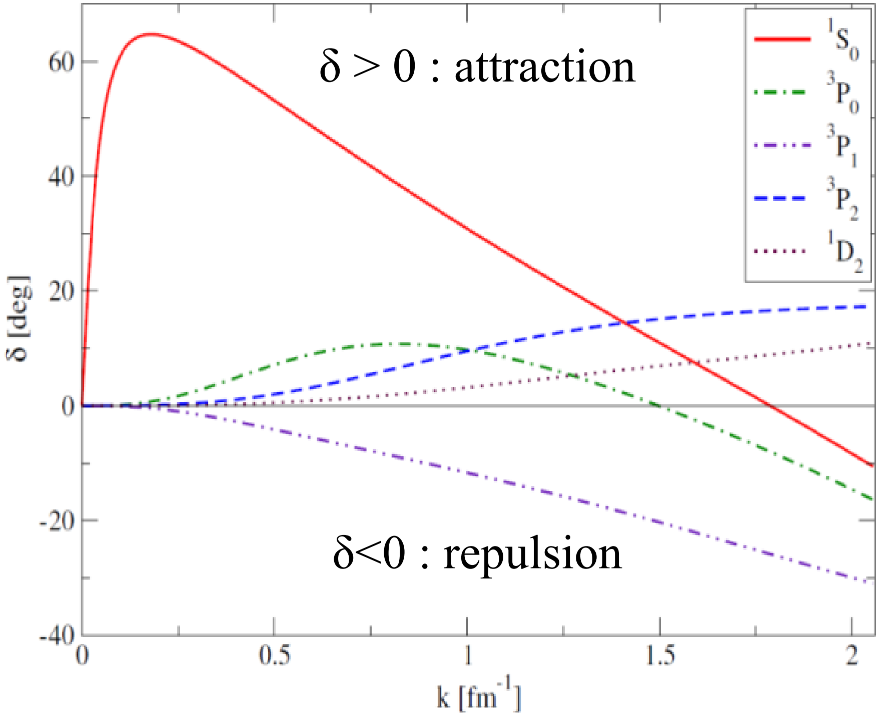

A. Gezerlis, *et al*, arXiv:1406.6109v2

Nucleon pairing gaps in unpolarized matter

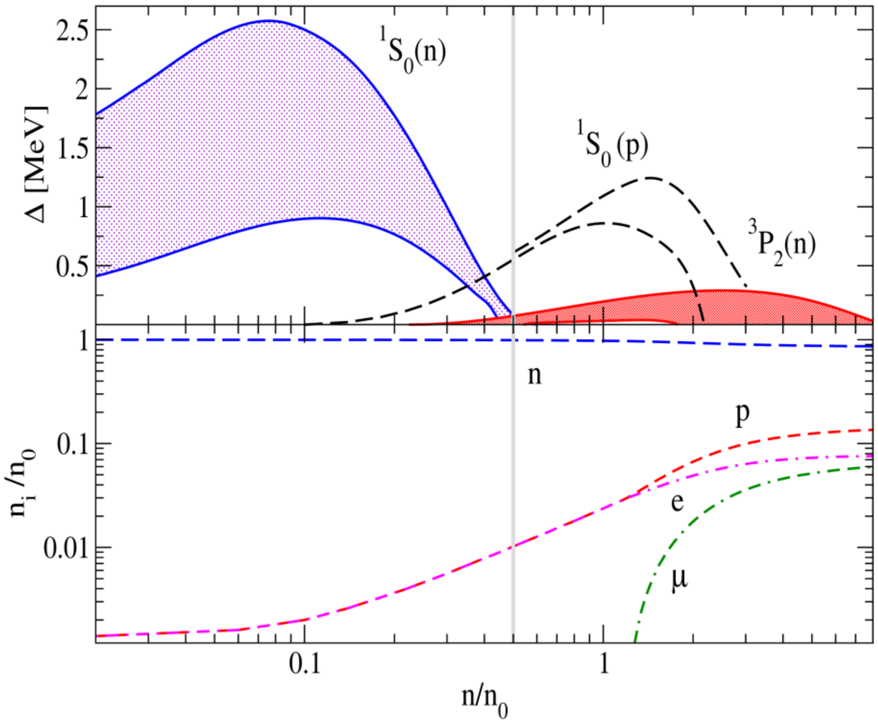

Eur. Phys. J. A (2019) **55**: 167

Today's talk

We address two questions from condensed-matter (cold-atomic) perspective

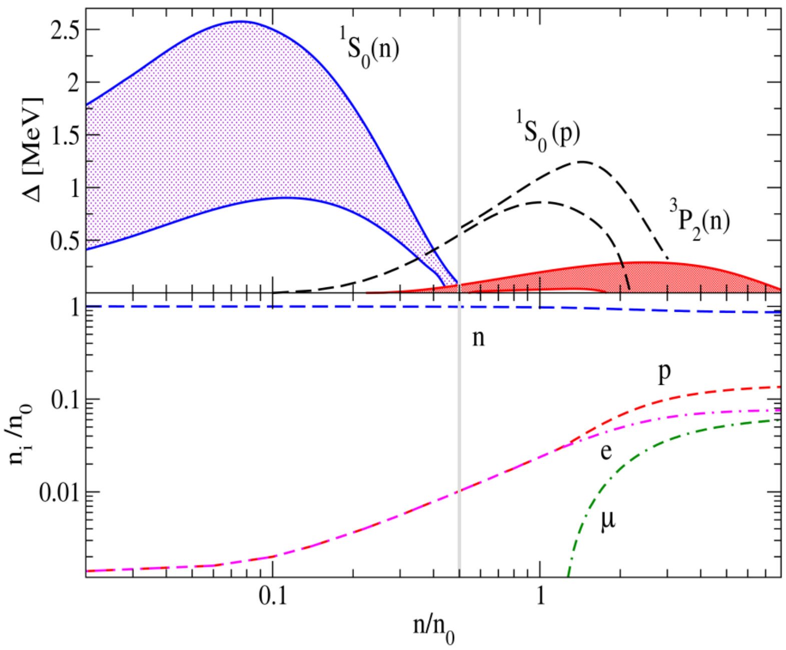

1: HT, H. Funaki, Y. Sekino, N. Yasutake, and M. Matsuo, Phys. Rev. C **108**, L052802 (2023).

2: Y. Guo, HT, T. Hatsuda, and H. Liang, Phys. Rev. A **108**, 023304 (2023).

Today's talk

We address two questions from condensed-matter (cold-atomic) perspective

1. At low-energy scattering, the $^3P_0$ channel is attractive ➡ **$^3P_0$ superfluid?**

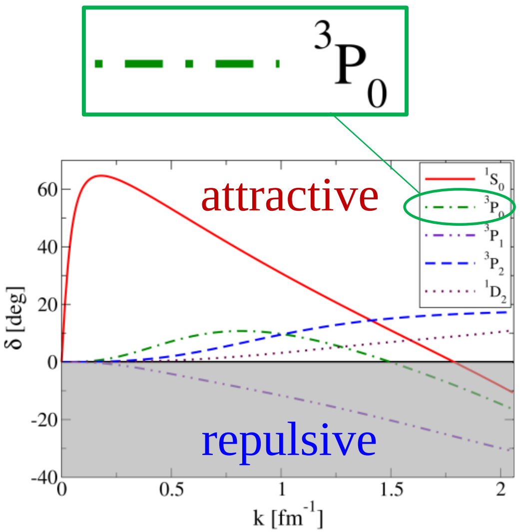

A. Gezerlis, *et al*,
arXiv:1406.6109v2

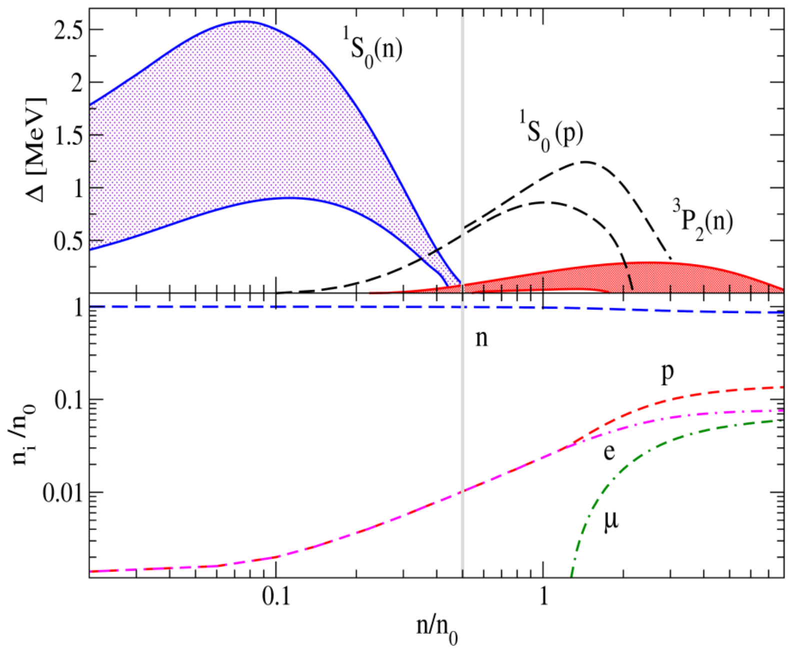

1: HT, H. Funaki, Y. Sekino, N. Yasutake, and M. Matsuo, Phys. Rev. C **108**, L052802 (2023).

Today's talk

We address two questions from condensed-matter (cold-atomic) perspective

1. At low-energy scattering, the $^3P_0$ channel is attractive ➡ **$^3P_0$ superfluid?**
2. $^3P_2$ neutron superfluid may change to quark one ➡ **Superfluid continuity?**

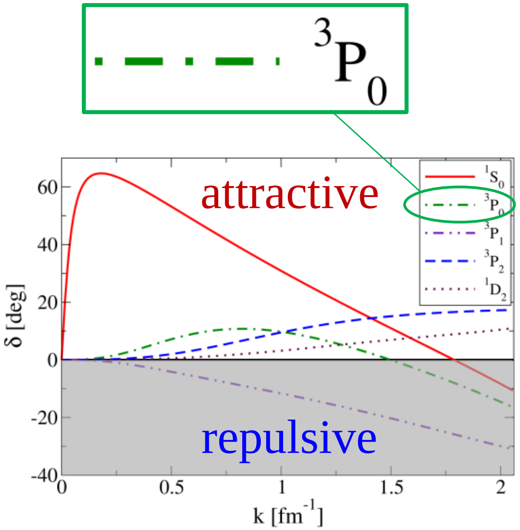

A. Gezerlis, *et al*, arXiv:1406.6109v2

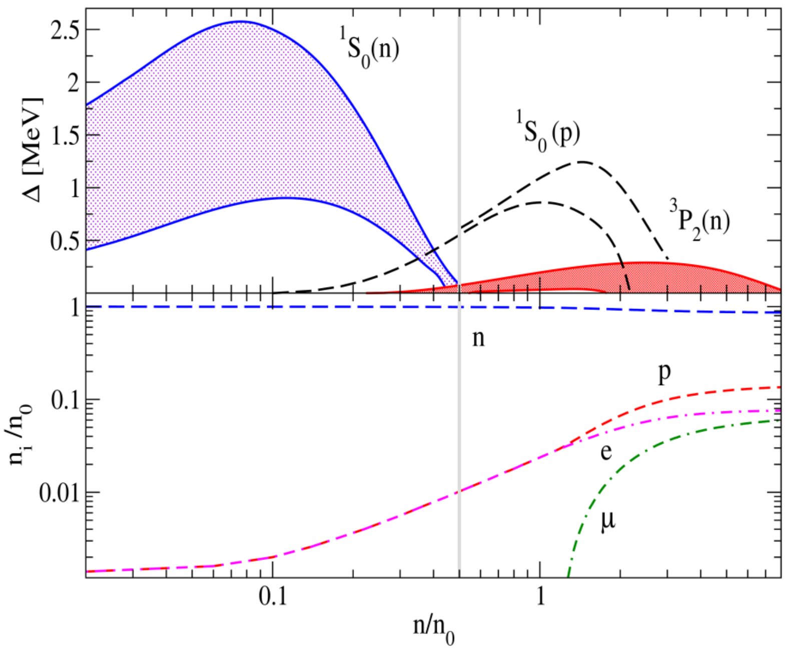

P-wave pairing of dinucleon and diquark

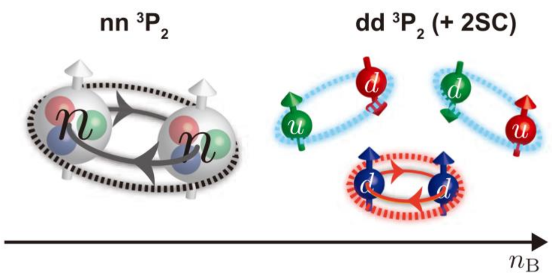

Yuki Fujimoto, et al., Phys. Rev. D **101**, 094009 (2020).

1: HT, H. Funaki, Y. Sekino, N. Yasutake, and M. Matsuo, Phys. Rev. C **108**, L052802 (2023).

2: Y. Guo, HT, T. Hatsuda, and H. Liang, Phys. Rev. A **108**, 023304 (2023).

Outline

- Brief introduction of neutron superfluid
- ${}^3P_0$ neutron superfluid at low density
- Fate of *P*-wave pairing at high density
- Summary

Outline

- Brief introduction of neutron superfluid
- $^3P_0$ neutron superfluid at low density
- Fate of P-wave pairing at high density
- Summary

Spin-singlet pairing

NN scattering phase shift

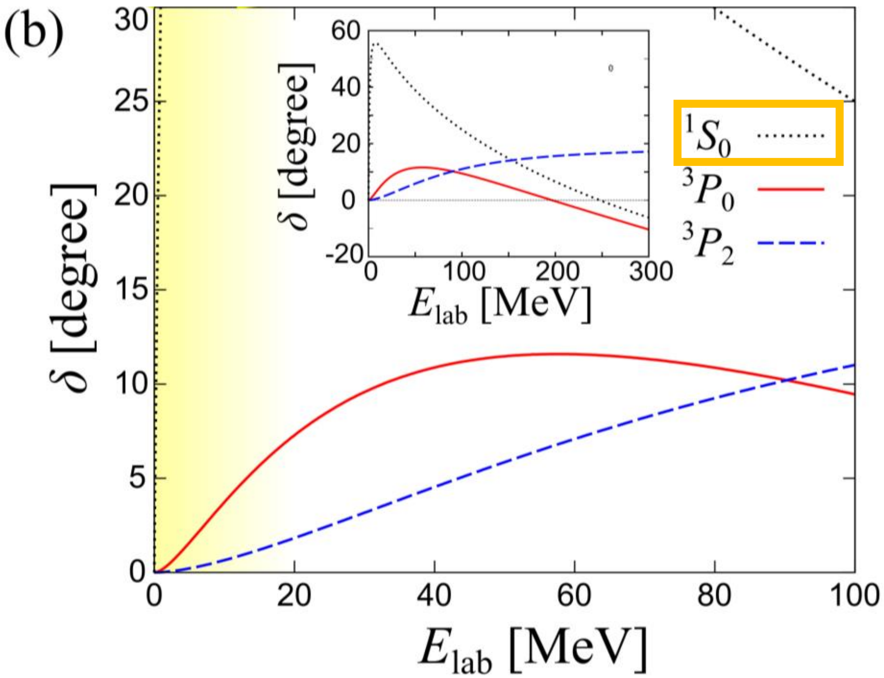

$^1S_0$ pairing (antiparallel spin)

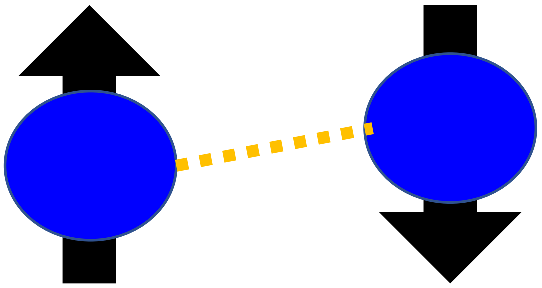

Spin-singlet pairing

NN scattering phase shift

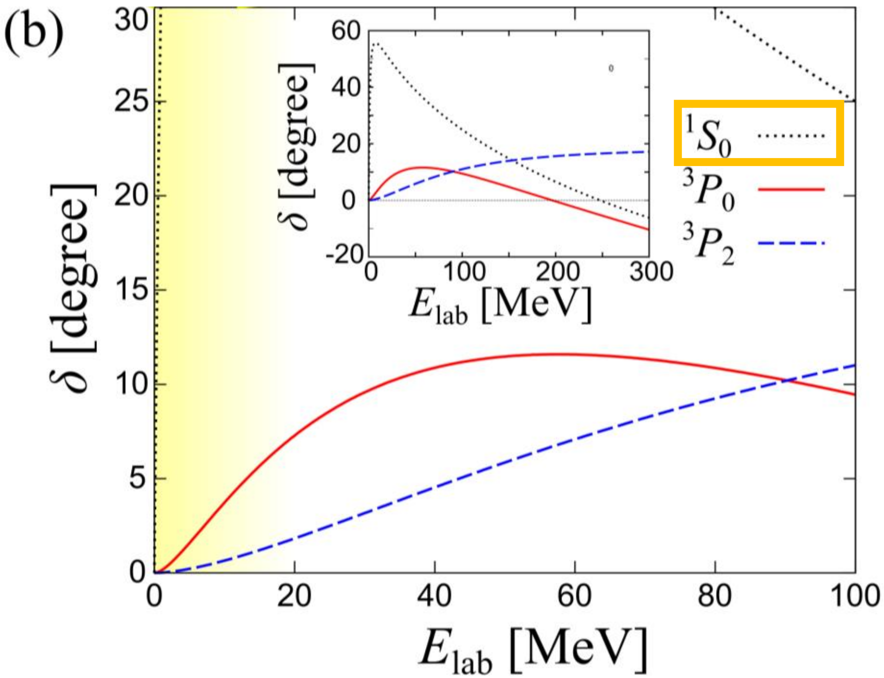

$^1S_0$ pairing (antiparallel spin)

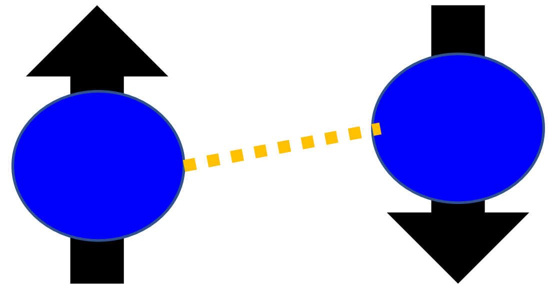

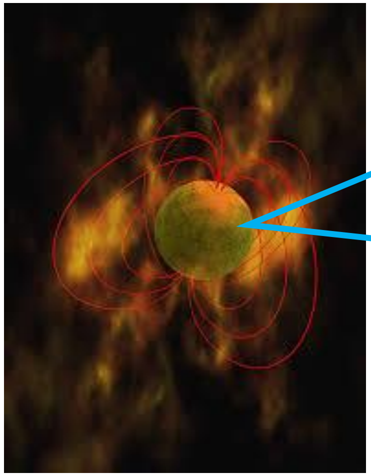

wikipedia

Destroyed in magnetar?

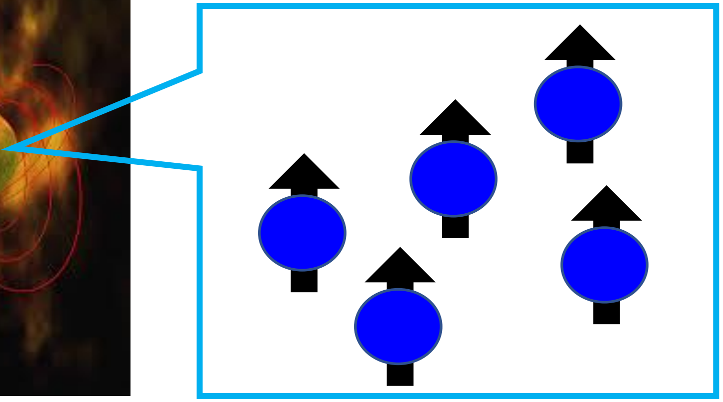

Magnetized neutron star

Strong magnetic field may affect neutron superfluid

Deformation indicates strong toroidal magnetic field

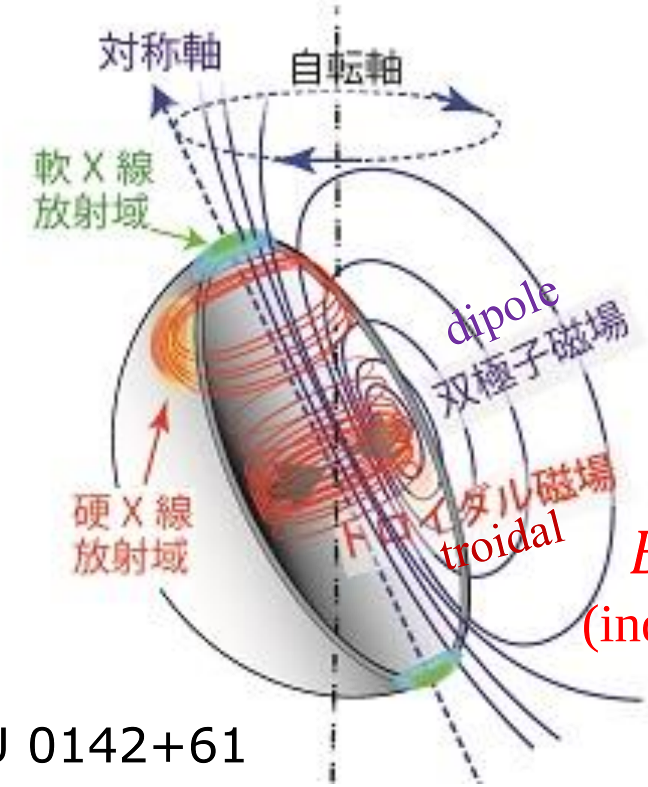

$B_d \sim 10^{14-15} G$
(directly observed)

$B_t \sim 10^{15-17} G$
(indirectly estimated)

4U 0142+61

K. Makishima, *et al.*, Phys. Rev. Lett. **112**, 171102 (2014).

Temperature profile (simulation)

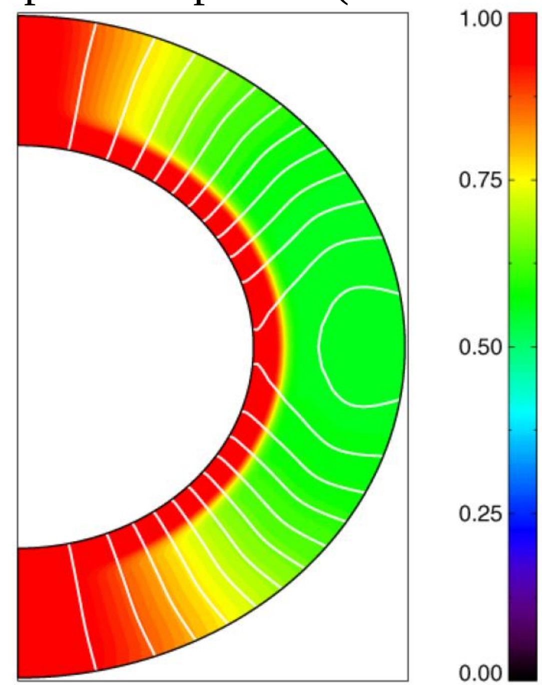

Fig. 5 Temperature distribution in a strongly magnetized neutron star crust (whose thickness has been stretched by a factor five for easier reading). The chosen field scale parameters are $B_0^{core} = 7.5 \times 10^{12}$ G, $B_0^{crust} = 2.5 \times 10^{12}$ G, $B_0^{tor} = 3 \times 10^{15}$ G, and the toroidal component's generating functions T is the model "T1" of Fig. 4. The color code maps the relative temperature, i.e., $T(r, \theta)/T_{core}$, with a core temperature $T_{core} = 6 \times 10^7$ K. *White lines* show field lines of $\mathbf{B}^{pol}$, the *field lines* of $\mathbf{B}^{tor}$ being perpendicular to the plane of the figure. The heat blanketing effect of the toroidal component is clearly visible. (From Geppert et al. 2006)

Astrophys Space Sci (2007) 308: 403–412

Zeeman shift of neutron energy

$$h = \frac{1}{2}|\gamma_n||\boldsymbol{B}|$$

$\gamma_n = -1.2 \times 10^{-17}$MeV/G: neutron gyromagnetic ratio

For $|B| = 10^{15-18}$ G, $h = 10^{-2} \sim 10$MeV $\ll E_{\mathrm{F}}(\rho = \rho_0)$

Zeeman shift of neutron energy

$$h = \frac{1}{2}|\gamma_n||\boldsymbol{B}|$$

$\gamma_n = -1.2 \times 10^{-17}$MeV/G: neutron gyromagnetic ratio

For $|B| = 10^{15-18}$ G, $h = 10^{-2} \sim 10\text{MeV} \ll E_{\text{F}}(\rho = \rho_0)$

Negligible for many-body properties around nuclear saturation density

Fermi energy at nuclear saturation density

$$E_{\text{F}}(\rho = \rho_0) = \frac{(3\pi^2\rho_0)^{2/3}}{2M} \simeq 60\text{MeV}$$

Zeeman shift of neutron energy

$$h = \frac{1}{2}|\gamma_n||\boldsymbol{B}|$$

$\gamma_n = -1.2 \times 10^{-17}\mathrm{MeV/G}$: neutron gyromagnetic ratio

For $|B| = 10^{15-18}$ G, $h = 10^{-2} \sim 10\mathrm{MeV} \ll E_{\mathrm{F}}(\rho = \rho_0)$

Negligible for many-body properties around nuclear saturation density

Fermi energy at nuclear saturation density

$$E_{\mathrm{F}}(\rho = \rho_0) = \frac{(3\pi^2\rho_0)^{2/3}}{2M} \simeq 60\mathrm{MeV}$$

However, it is not the case for dilute neutron matter

Fermi energy around neutron drip density

$$E_{\mathrm{F}}(\rho = 10^{-3}\rho_0) = \frac{(3\pi^2 \times 10^{-3}\rho_0)^{2/3}}{2M} \simeq 0.6\mathrm{MeV} \sim h$$

$^3P_0$ pairing in dilute neutron matter under the strong magnetic field

Spin-triplet pairing can survive even under the strong magnetic field

+

The attractive $^3P_0$ channel is stronger than the $^3P_2$ one up to $E_{\rm lab} \simeq 90$MeV

=

$^3P_0$ superfluid at low densities under the strong magnetic field?

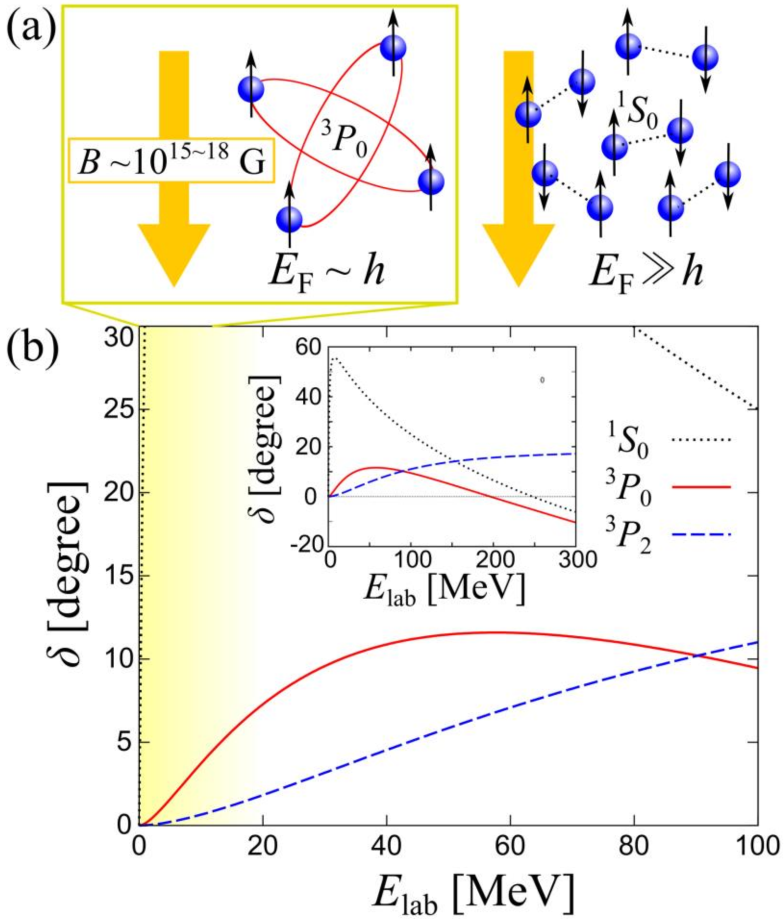

$E_{\rm lab} \simeq 4E_F(\rho)$

Properties of dilute neutron matter and ultracold Fermi gases

- The low-density neutron matter can be mimicked by an ultracold Fermi gas

Phase shift (effective range expansion)

$$k\cot\delta_k = -\frac{1}{a_s} + \frac{1}{2}k^2 r_\mathrm{e}$$

a_s: s-wave scattering length

r_e: effective range

	Cold atom	Neutrons
a_s	$-\infty \sim \infty$	-18.5 fm
r_eff	~ 0	2.8 fm
density	$\sim 10^{15}\ \mathrm{cm}^{-3}$	$\sim 0.17\ \mathrm{fm}^{-3}$
$(k_\mathrm{F} a_s)^{-1}$	$-\infty \sim \infty$	$-\infty \sim 0$

Phase shift of NN scattering

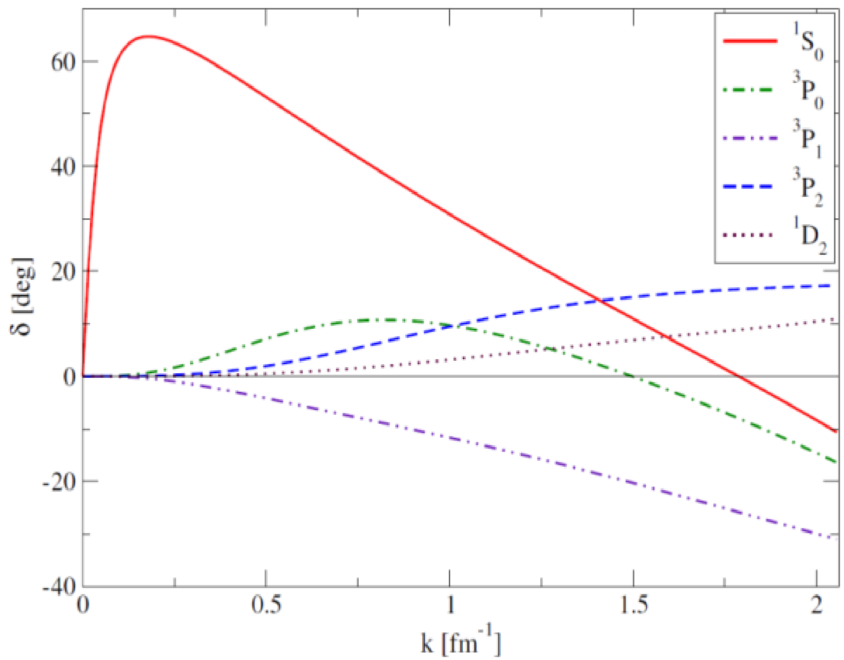

A. Gezerlis, *et al*, arXiv : 1406.6109v2

$*$ k_F: Fermi momentum

Atomic Fermi gas and neutron matter

- The low-density neutron matter can be mimicked by an ultracold Fermi gas

M. Horikoshi, M. Koashi, HT, Y. Ohashi, and M. Kuwata-Gonokami, PRX, **7**, 041004 (2017).

Precise measurement of cold atom EOS

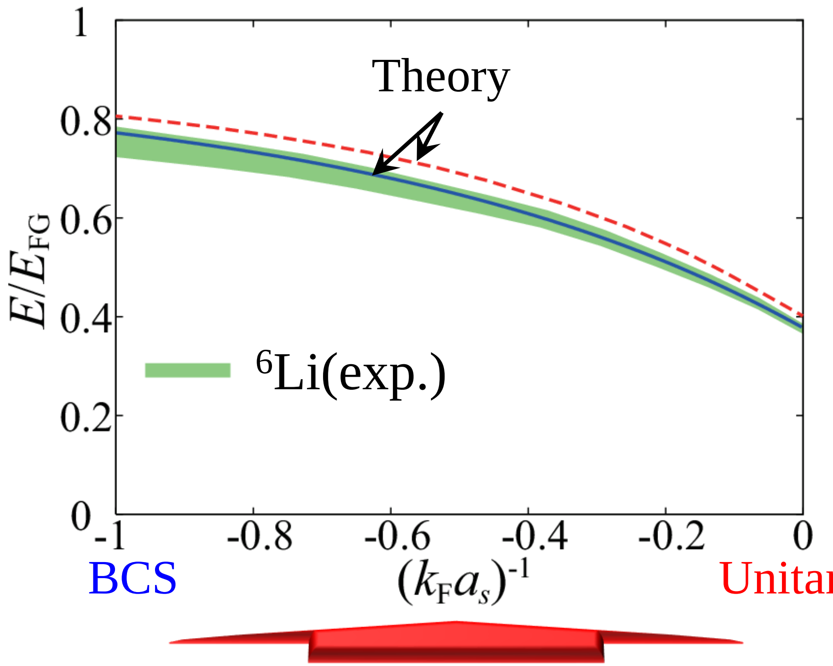

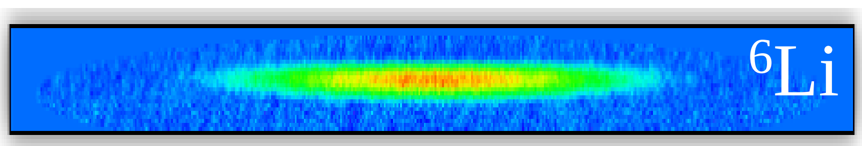

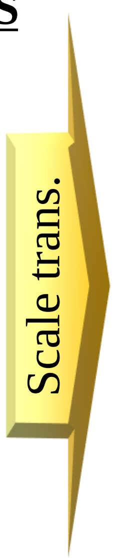

EOS of neutron matter and cold atom

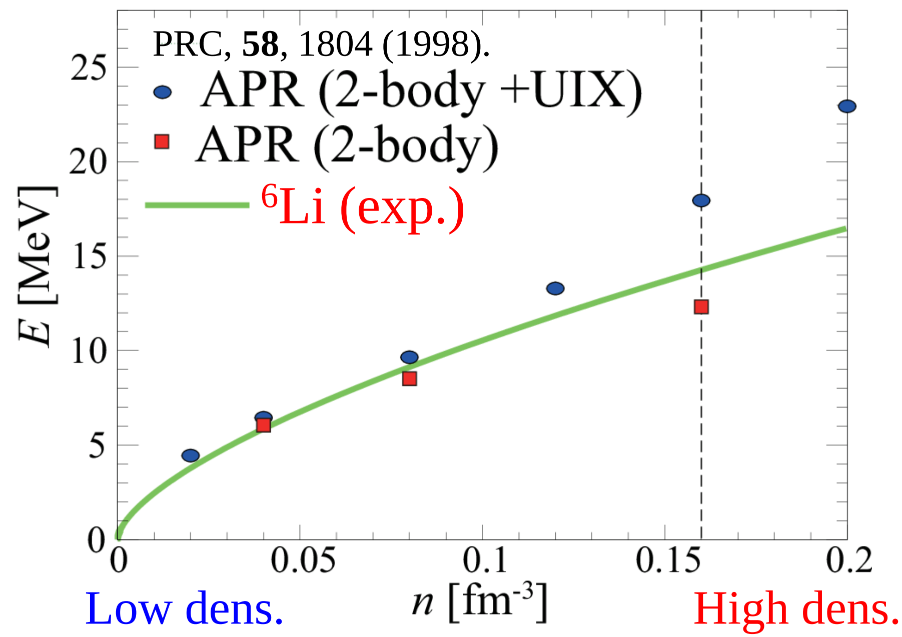

Agreement in the low density region

When is a Fermi gas fully spin-polarized?

When spin down neutrons start to be occupied ➡ saturation Zeeman shift h_s

Non-interacting case

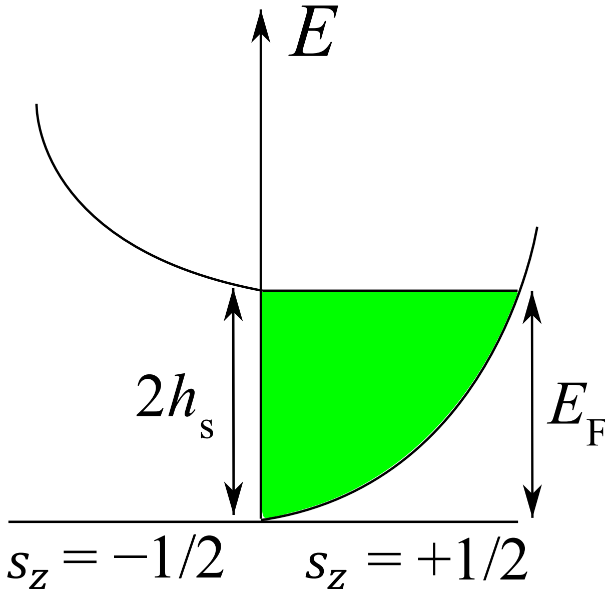

$$h_s = \frac{E_F}{2}$$

Attractively-interacting case

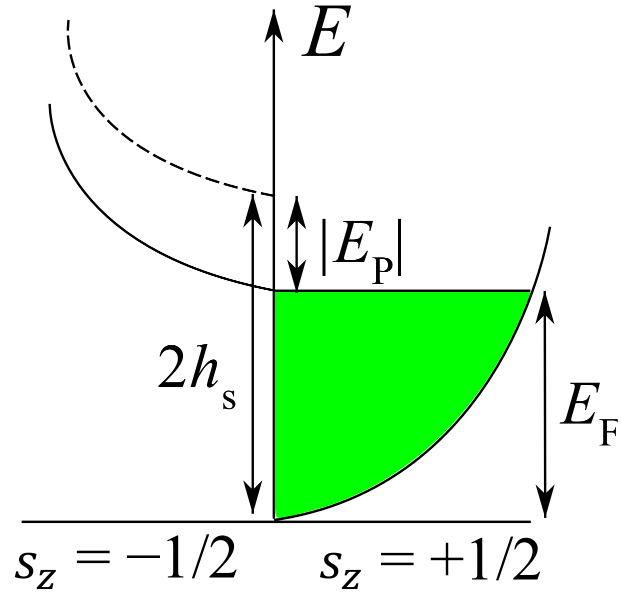

$$h_s = \frac{E_F + |E_P|}{2}$$

E_P: Fermi polaron energy

(energy gain by dressing majority components)

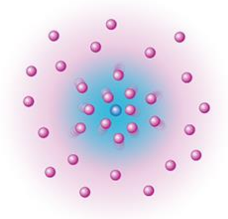

Attractive Fermi-polaron energy

Fermi polaron energy has been studied in strongly interacting Fermi gases

G-matrix calculation of Fermi polaron energy (2D)

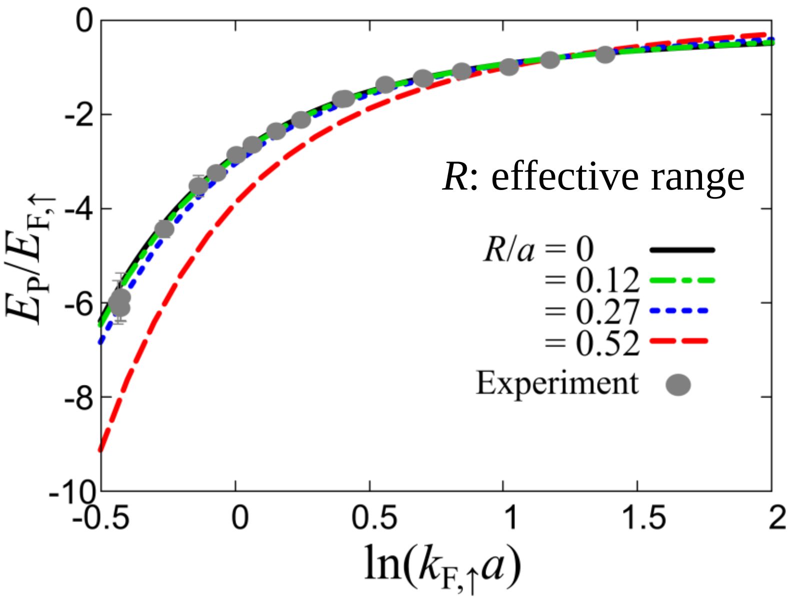

H. Sakakibara, HT, and H. Liang, Phys. Rev. A **107**, 053313 (2023)

Fermi polaron energy (G-matrix calculation in 3D)

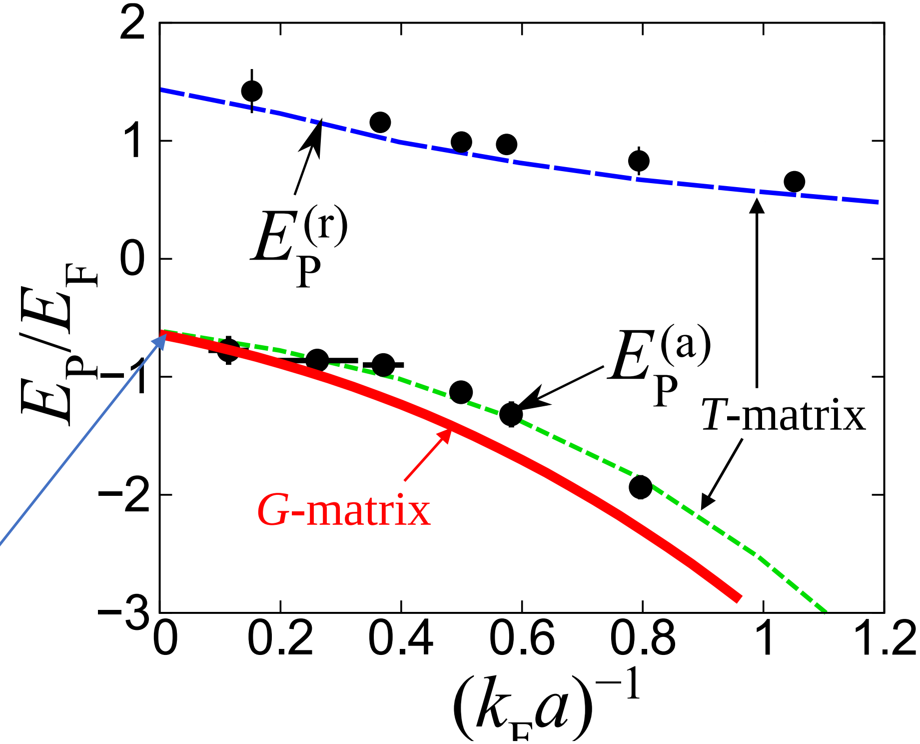

Exp.: F. Scazza, et al., Phys. Rev. Lett. **118**, 083602 (2017).

T-matrix: HT and S. Uchino, NJP, **20**, 073048 (2018).

$E_P = -0.64(7)E_F$ Exp. at unitarity: PRL **102**, 230402 (2009).

Possible ground-state phase diagram

$$h = \frac{1}{2}|\gamma_n||\boldsymbol{B}|$$

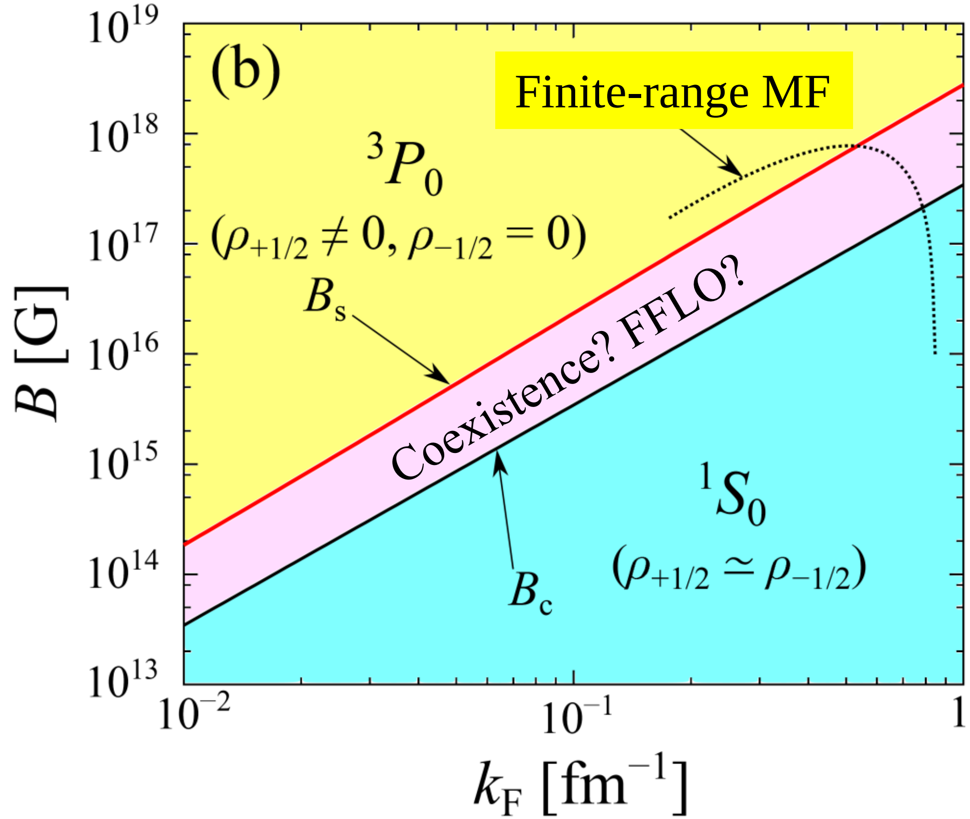

Critical magnetic field

$$h_c \simeq 1.09\mu_c$$
$$\simeq 1.09 \times 0.37 E_F$$

Bertsch parameter

PRX, **7**, 041004 (2017).

Saturation Zeeman shift

$$h_s = \frac{E_F + |E_P|}{2}$$

Attractive Fermi polaron energy (*G*-matrix calculation)

$$E_P = \frac{\rho_{+1/2}}{\frac{M}{4\pi a} - \frac{Mk_F}{2\pi^2}} = -\frac{2}{3}E_F \frac{1}{1 - \frac{\pi}{2}(k_F a)^{-1}} \quad (a < 0)$$

Neutron-neutron scattering length : $a = -18.5$ fm

Estimation of the critical temperature

$^3P_0$ *NN* interaction

$$V_{^3P_0} = 2\pi \sum_{\boldsymbol{k},\boldsymbol{k}',\boldsymbol{P}} \sum_{m} \sum_{S_z} \sum_{s_z, s'_z} V(k,k') Y_{1,m}(\hat{\boldsymbol{k}}) Y^*_{1,m}(\hat{\boldsymbol{k}}')$$
$$\times \langle 1, m; 1, S_z | 0, J_z \rangle^2 \langle s, s_z; s, s_z | 1, S_z \rangle^2$$
$$\times c^\dagger_{\boldsymbol{k}+\boldsymbol{P}/2, s_z} c^\dagger_{-\boldsymbol{k}+\boldsymbol{P}/2, s'_z} c_{-\boldsymbol{k}'+\boldsymbol{P}/2, s'_z} c_{\boldsymbol{k}'+\boldsymbol{P}/2, s_z},$$

$c^{(\dagger)}_{\boldsymbol{k}, s_z}$: neutron annihilation (creation) operator

Scattering volume, effective range

$$v = -2.638 \ \mathrm{fm}^3 \qquad r = 3.182 \ \mathrm{fm}^{-1}$$

Phys. Rev. C **82**, 034003 (2010).

Separable interaction: $V(k,k') = g\gamma_k \gamma_{k'}$

Form factor: $\gamma_k = \frac{k}{1+(k/\Lambda)^2}$

$$v^{-1} = \frac{12\pi}{M}\left(\frac{1}{g} + \frac{M_\nu \Lambda^3}{24\pi}\right),$$

$$r = -\frac{24\pi}{M}\left(\frac{2}{g\Lambda^2} + \frac{M\Lambda}{8\pi}\right) = -\frac{48\pi}{gM\Lambda^2} - 3\Lambda$$

BCS-Leggett theory for $^3P_0$ superfluid

Mean-field Hamiltonian

$$H_{\mathrm{MF}} = \frac{1}{2}\sum_{\boldsymbol{k}} \Psi_{\boldsymbol{k}}^{\dagger} \begin{pmatrix} \xi_{\boldsymbol{k},+1/2} & -\Delta_{\boldsymbol{k}} \\ -\Delta_{\boldsymbol{k}}^{*} & -\xi_{\boldsymbol{k},+1/2} \end{pmatrix} \Psi_{\boldsymbol{k}} - \frac{|d|^2}{2g^2} + \frac{1}{2}\sum_{\boldsymbol{k}} \xi_{\boldsymbol{k},+1/2},$$

Pairing gap

$$\Delta_{\boldsymbol{k}} = \gamma_k \frac{k_x - ik_y}{\sqrt{2}k} d,$$

$$d = -g\sum_{\boldsymbol{q}} \frac{q_x + iq_y}{\sqrt{2}q} \gamma_q \langle c_{-\boldsymbol{q},1/2} c_{\boldsymbol{q},1/2} \rangle$$

***T*$_{\mathrm{c}}$ equation**

$$1 = -\frac{Mg}{6\pi^2}\int_0^{\infty} q^2 dq \frac{\gamma_q^2}{2M\xi_{\boldsymbol{q},+1/2}} \tanh\left(\frac{\xi_{\boldsymbol{q},+1/2}}{2T_{\mathrm{c}}}\right)$$

Neutron number density

$$\rho_{+1/2} = \frac{1}{4\pi^2}\int_0^{\infty} k^2 dk \left[1 - \tanh\left(\frac{\xi_{\boldsymbol{k},+1/2}}{2T_{\mathrm{c}}}\right)\right]$$

$^3P_0$ superfluid critical temperature

It is still elusive whether astrophysical environments satisfying the condition for $^3P_0$ superfluid exist or not in nature.

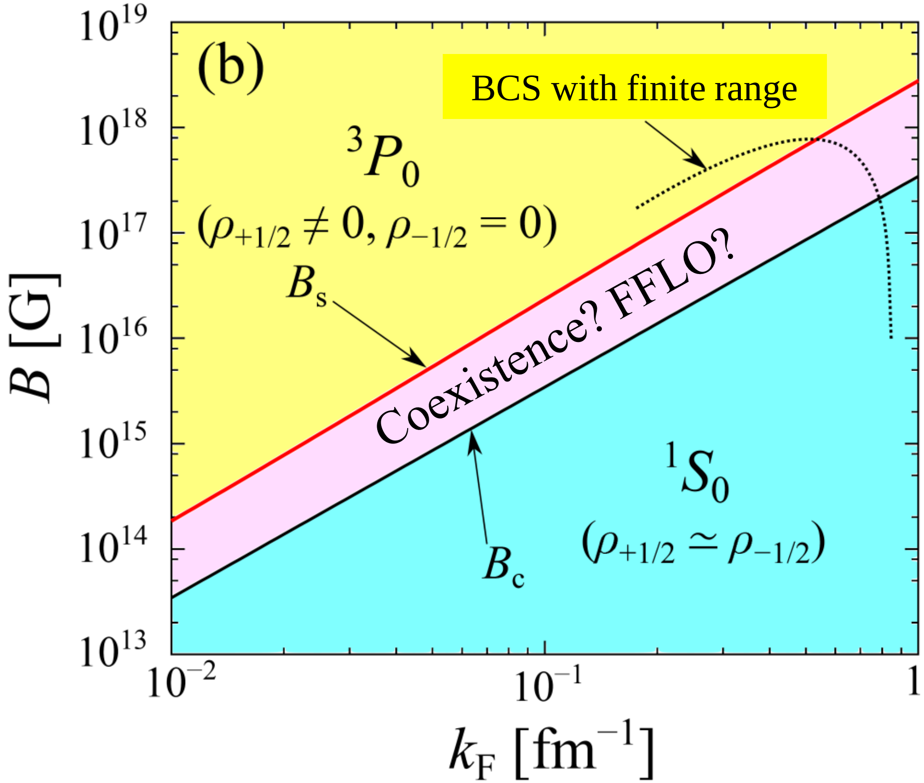

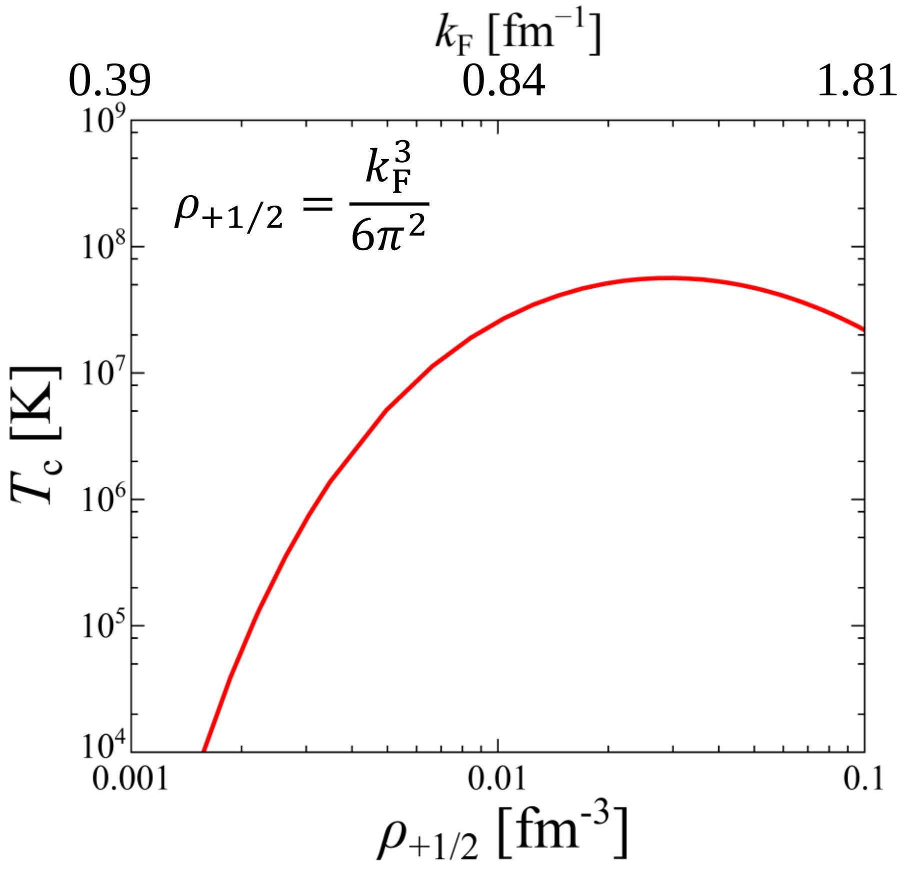

$^3P_0$ superfluid critical temperature

It is still elusive whether astrophysical environments satisfying the condition for $^3P_0$ superfluid exist or not in nature. A possible candidate is **the surface region of the magnetar with a strong toroidal magnetic field**.

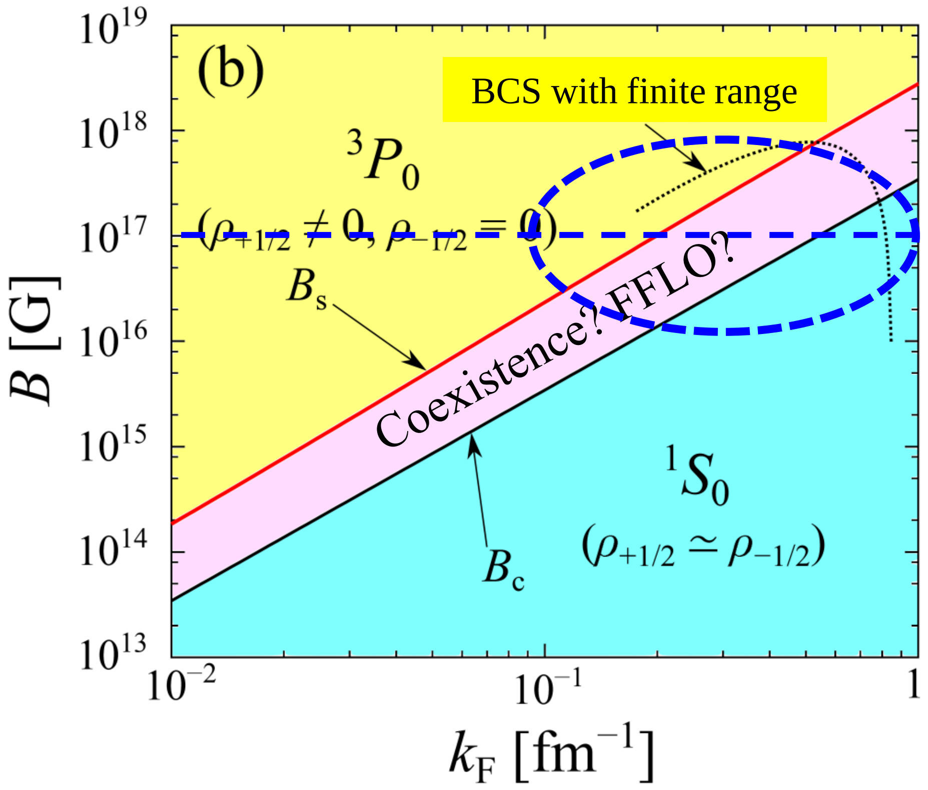

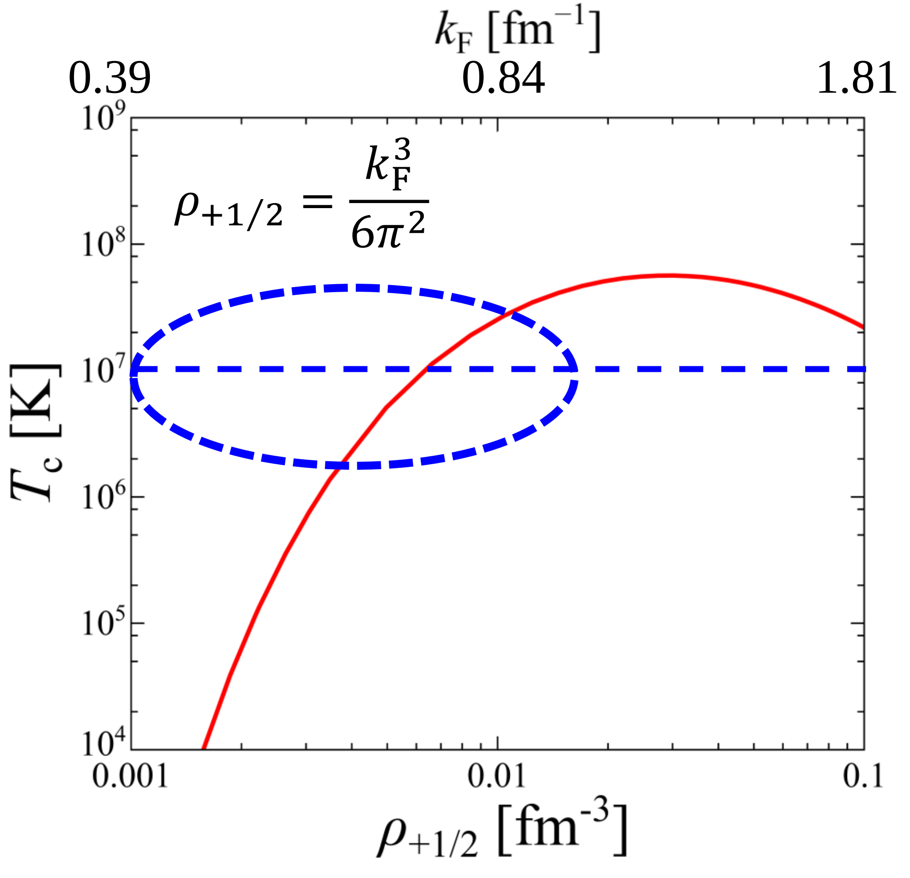

Topological properties of $^3P_0$ superfluid

Similar to p_x+ip_y Fermi superfluid and A_1 phase of ^{3}He superfluid

Pairing gap

$$\Delta_{\boldsymbol{k}} = \gamma_k \frac{k_x - i k_y}{\sqrt{2}k} d,$$

Quasiparticle dispersion

$$E_{\boldsymbol{k}} \quad = \quad \sqrt{\xi^2_{\boldsymbol{k},+1/2} + |\Delta_{\boldsymbol{k}}|^2}$$

Weyl nodes

$\mathbf{p}_1 = (0, 0, p_F)$

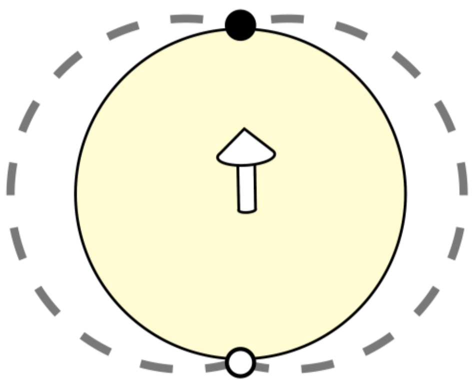

$\mathbf{p}_2 = (0, 0, -p_F)$

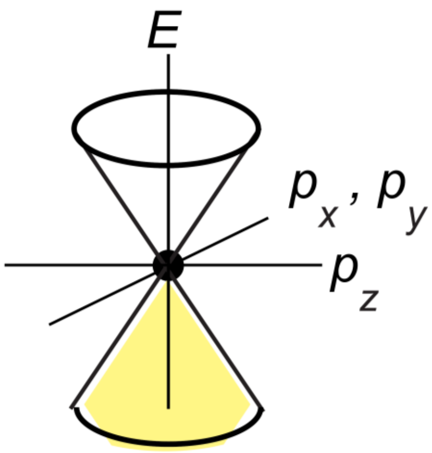

G. E. Volovik, Lect. Notes Phys.718:31-73, (2007).

Outline

- Brief introduction of neutron superfluid
- $^3P_0$ neutron superfluid at low density
- Fate of *P*-wave pairing at high density
- Summary

Outline

- Brief introduction of neutron superfluid
- $^3P_0$ neutron superfluid at low density
- Fate of *P*-wave pairing at high density
- Summary

Simulating dense QCD matter with Bose-Fermi mixture

Molecule≃ Nucleon   Fermi atom ≃ Quark   Bose atom ≃ Diquark

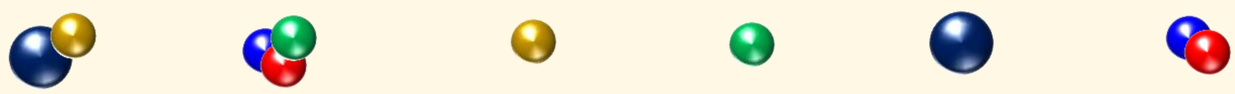

Schematic phase diagram

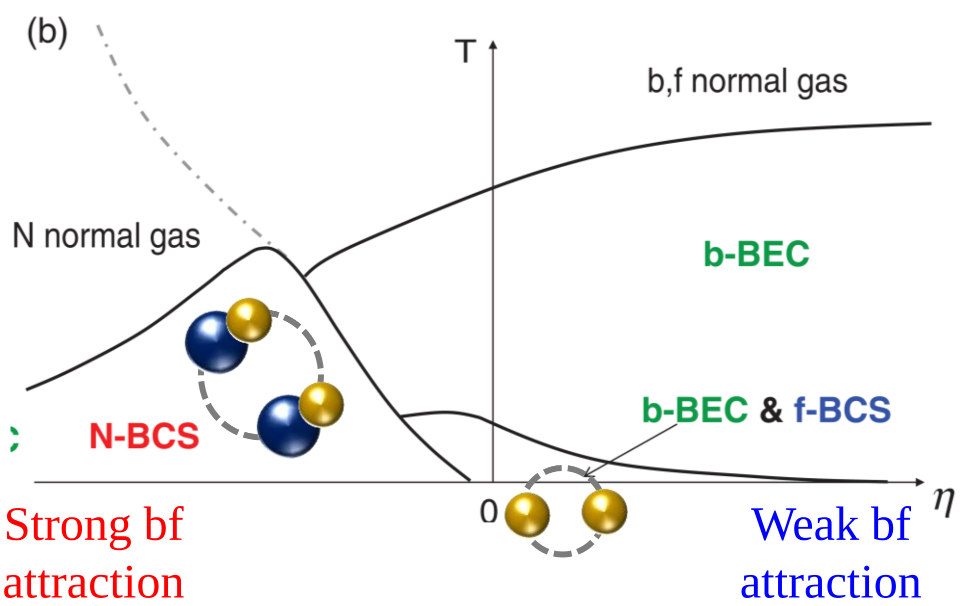

K. Maeda, G. Baym, and T. Hatsuda, PRL **103**, 085301 (2009)

Recent experiment of ^{40}K-^{87}Rb mixture

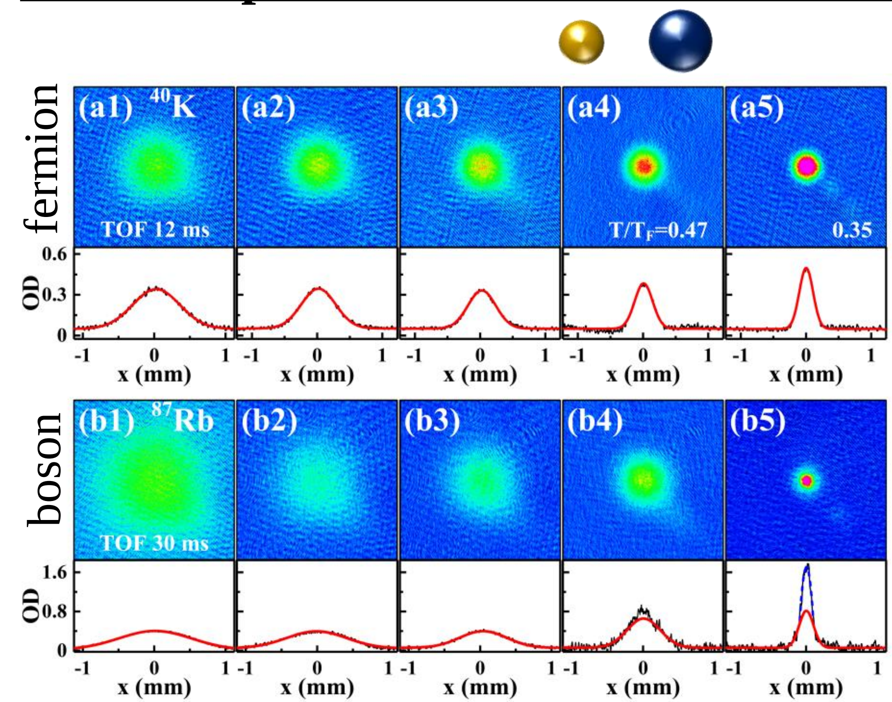

P. Ding, et al., CPC 10.1088/1674-1056/ad334d

Is the continuity between atom and molecular superfluids possible?

K. Maeda, et al., PRL **103**, 085301 (2009)

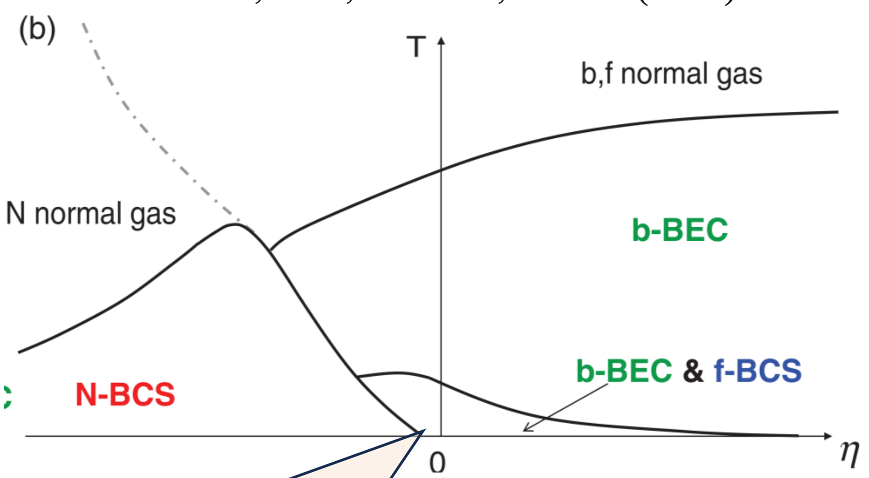

≈

K. Fukushima, *et al.*, Rep. Prog. Phys. **74**, 014001 (2011).

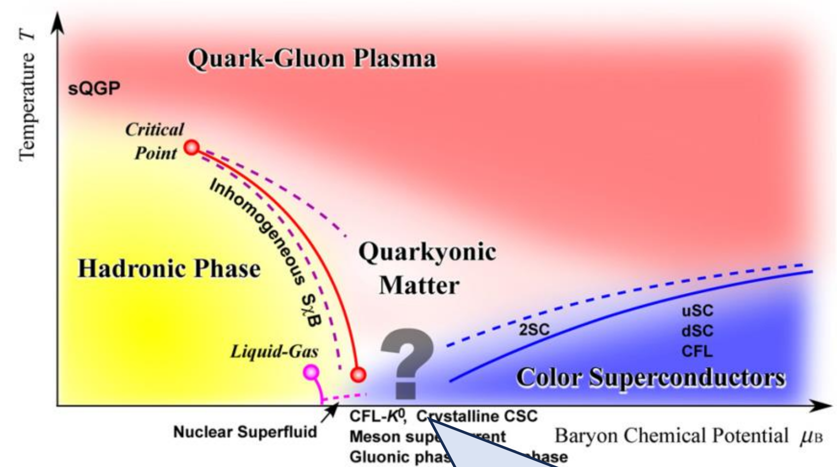

Molecule-molecule
***P*-wave pairing**

Atom-atom
***P*-wave pairing**

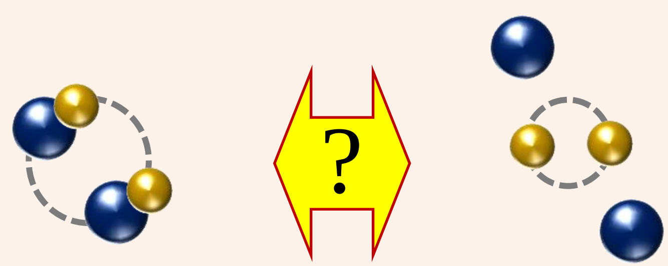

≈

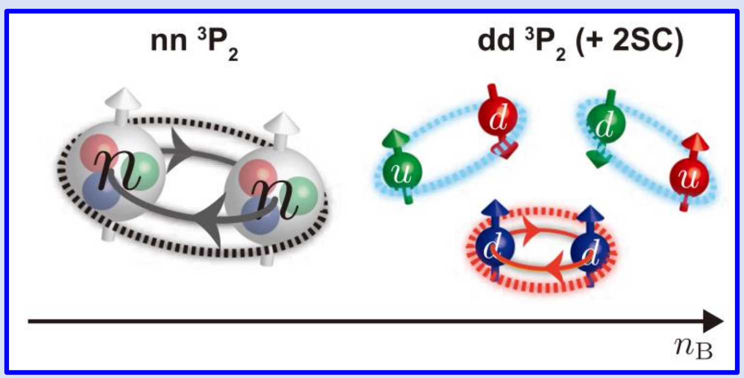

Yuki Fujimoto, et al., Phys. Rev. D **101**, 094009 (2020).

Hamiltonian of Bose-Fermi mixture

Total Hamiltonian: $H = H_{\text{Bose}} + H_{\text{Fermi}} + V_{Fbf}$

Bosonic part

$$H_{\text{Bose}} = K_b + V_{bb}$$

Fermionic part

$$H_{\text{Fermi}} = K_f + V_{ff} + K_F + V_{FF}$$

Hamiltonian of Bose-Fermi mixture

Total Hamiltonian: $H = H_{\text{Bose}} + H_{\text{Fermi}} + V_{Fbf}$

Bosonic part

$$H_{\text{Bose}} = \boxed{K_b} + V_{bb}$$

Fermionic part

$$H_{\text{Fermi}} = \boxed{K_f} + V_{ff} + \boxed{K_F} + V_{FF}$$

Kinetic terms

Bose atom (b)

$$K_b = \sum_{\boldsymbol{p}} \varepsilon_{\boldsymbol{p},b} b^\dagger_{\boldsymbol{p}} b_{\boldsymbol{p}}$$

Fermi atom (f)

$$K_f = \sum_{\boldsymbol{p}} \varepsilon_{\boldsymbol{p},f} f^\dagger_{\boldsymbol{p}} f_{\boldsymbol{p}},$$

Closed-channel molecule (F)

$$K_F = \sum_{\boldsymbol{p}} \varepsilon_{\boldsymbol{p},F} F^\dagger_{\boldsymbol{p}} F_{\boldsymbol{p}},$$

Dispersion relations

$$\varepsilon_{\boldsymbol{p},i} = \frac{p^2}{2m_i} - \mu_i \quad (i = b, f, F)$$

Chemical potentials

$$\mu_F = \mu_f + \mu_b - \nu_F \equiv \mu_f - \tilde{\nu}_F$$

ν_F: Closed-channel energy level

Hamiltonian of Bose-Fermi mixture

Total Hamiltonian: $H = H_{\rm Bose} + H_{\rm Fermi} + V_{Fbf}$

Bosonic part

$$H_{\rm Bose} = K_b + V_{bb}$$

Fermionic part

$$H_{\rm Fermi} = K_f + V_{ff} + K_F + V_{FF}$$

Interaction terms

Fermion-fermion interaction

$$V_{ff} = \frac{1}{2}\sum_{\boldsymbol{k},\boldsymbol{k}',\boldsymbol{q}} U_{ff}(\boldsymbol{k},\boldsymbol{k}') f^\dagger_{\boldsymbol{k}+\boldsymbol{q}/2} f^\dagger_{-\boldsymbol{k}+\boldsymbol{q}/2} f_{-\boldsymbol{k}'+\boldsymbol{q}/2} f_{\boldsymbol{k}'+\boldsymbol{q}/2}$$

Molecule-Molecule interaction

$$V_{FF} = \frac{1}{2}\sum_{\boldsymbol{k},\boldsymbol{k}',\boldsymbol{q}} U_{FF}(\boldsymbol{k},\boldsymbol{k}') F^\dagger_{\boldsymbol{k}+\boldsymbol{q}/2} F^\dagger_{-\boldsymbol{k}+\boldsymbol{q}/2} F_{-\boldsymbol{k}'+\boldsymbol{q}/2} F_{\boldsymbol{k}'+\boldsymbol{q}/2}$$

Boson-boson interaction

$$V_{bb} = \frac{1}{2} g_{bb} \sum_{\boldsymbol{P},\boldsymbol{q},\boldsymbol{q}'} b^\dagger_{\boldsymbol{P}/2+\boldsymbol{q}} b^\dagger_{\boldsymbol{P}/2-\boldsymbol{q}} b_{\boldsymbol{P}/2-\boldsymbol{q}'} b_{\boldsymbol{P}/2+\boldsymbol{q}'}$$

Feshbach resonance

$$V_{Fbf} = \sum_{\boldsymbol{P},\boldsymbol{q}} g(F^\dagger_{\boldsymbol{P}} b_{\boldsymbol{P}/2-\boldsymbol{q}} f_{\boldsymbol{P}/2+\boldsymbol{q}} + {\rm H.c.})$$

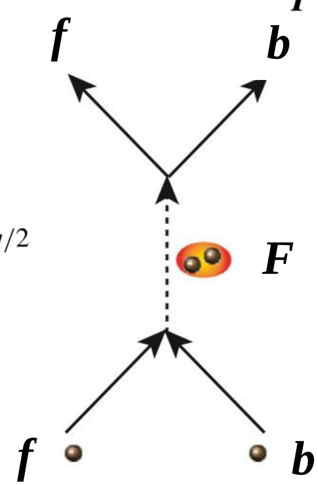

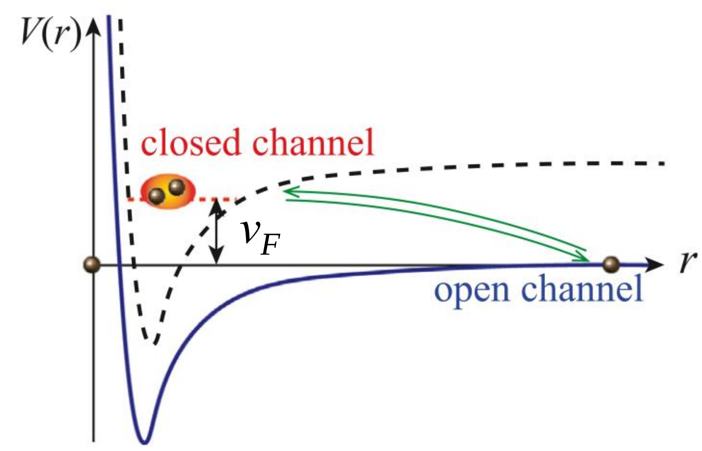

Y. Ohashi, HT, and P. van Wyk, Prog. Part. Nucl. Phys. **111**, 103739 (2020).

Effective interactions at leading order of the Feshbach coupling g

Assuming the Bose-Einstein condensate at low temperature: $\langle b_{\mathbf{0}} \rangle = \langle b_{\mathbf{0}}^{\dagger} \rangle = \sqrt{\rho_b}$

Global symmetry: $U(1)_f \times U(1)_F \times U(1)_b \xrightarrow{\text{Feshbach}} U(1)_{f+F} \times U(1)_b \xrightarrow{\text{BEC}} U(1)_{f+F}$

Effective interactions at leading order of the Feshbach coupling g

Assuming the Bose-Einstein condensate at low temperature: $\langle b_{\mathbf{0}} \rangle = \langle b_{\mathbf{0}}^{\dagger} \rangle = \sqrt{\rho_b}$

Global symmetry: $U(1)_f \times U(1)_F \times U(1)_b \xrightarrow{\text{Feshbach}} U(1)_{f+F} \times U(1)_b \xrightarrow{\text{BEC}} U(1)_{f+F}$

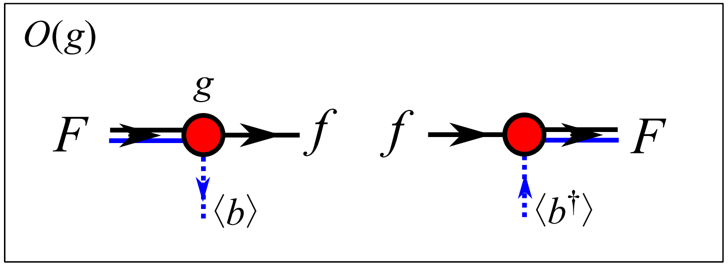

<u>One-body mixing</u>

$$V_{\mathrm{M}} = g\sqrt{\rho_b}\sum_{\boldsymbol{P}}(F_{\boldsymbol{P}}^{\dagger} f_{\boldsymbol{P}} + f_{\boldsymbol{P}}^{\dagger} F_{\boldsymbol{P}})$$

Effective interactions at leading order of the Feshbach coupling g

Assuming the Bose-Einstein condensate at low temperature: $\langle b_{\mathbf{0}} \rangle = \langle b_{\mathbf{0}}^{\dagger} \rangle = \sqrt{\rho_b}$

Global symmetry: $U(1)_f \times U(1)_F \times U(1)_b \xrightarrow{\text{Feshbach}} U(1)_{f+F} \times U(1)_b \xrightarrow{\text{BEC}} U(1)_{f+F}$

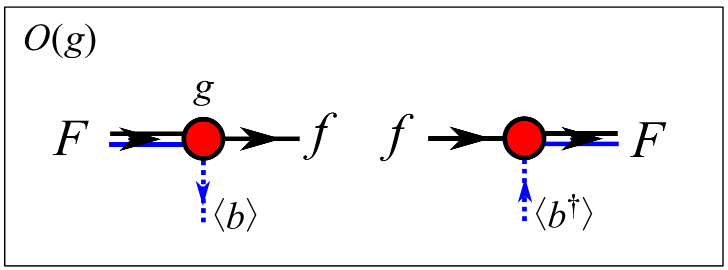

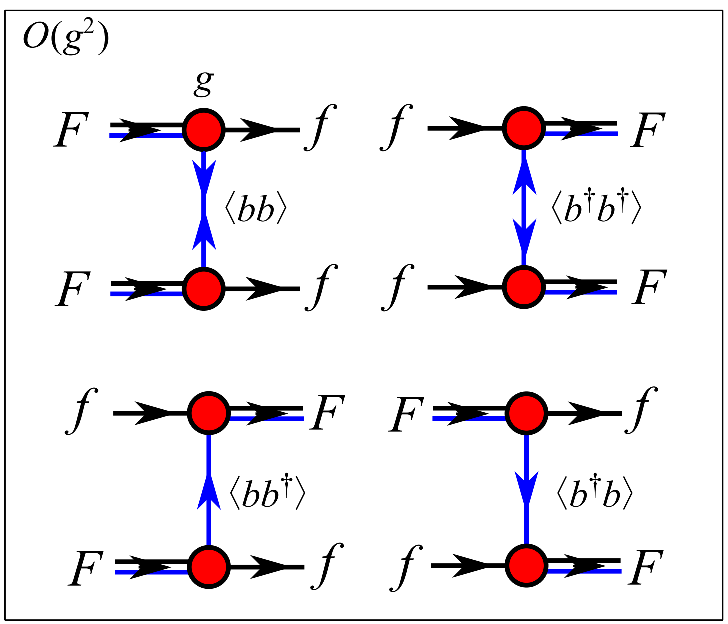

One-body mixing

$$V_{\mathrm{M}} = g\sqrt{\rho_b} \sum_{\boldsymbol{P}} (F_{\boldsymbol{P}}^{\dagger} f_{\boldsymbol{P}} + f_{\boldsymbol{P}}^{\dagger} F_{\boldsymbol{P}})$$

Pair-exchange coupling

$$V_{\mathrm{SMW}} = \frac{1}{2} \sum_{\boldsymbol{k},\boldsymbol{k}',\boldsymbol{P}} U_{\mathrm{SMW}}(\boldsymbol{q}, \omega) \times f_{\boldsymbol{k}+\boldsymbol{P}/2}^{\dagger} f_{-\boldsymbol{k}+\boldsymbol{P}/2}^{\dagger} F_{-\boldsymbol{k}'+\boldsymbol{P}/2} F_{\boldsymbol{k}'+\boldsymbol{P}/2} + \text{H.c.},$$

Boson-exchange coupling

$$V_{\mathrm{PM}} = \frac{1}{2} \sum_{\boldsymbol{k},\boldsymbol{k}',\boldsymbol{P}} U_{\mathrm{PM}}(\boldsymbol{q}, \omega) \times F_{\boldsymbol{k}+\boldsymbol{P}/2}^{\dagger} F_{-\boldsymbol{k}'+\boldsymbol{P}/2} f_{-\boldsymbol{k}+\boldsymbol{P}/2}^{\dagger} f_{\boldsymbol{k}'+\boldsymbol{P}/2} + \text{H.c.},$$

Effective interactions at leading order of the Feshbach coupling g

Assuming the Bose-Einstein condensate at low temperature: $\langle b_{\mathbf{0}} \rangle = \langle b_{\mathbf{0}}^{\dagger} \rangle = \sqrt{\rho_b}$

Global symmetry: $U(1)_f \times U(1)_F \times U(1)_b \xrightarrow{\text{Feshbach}} U(1)_{f+F} \times U(1)_b \xrightarrow{\text{BEC}} U(1)_{f+F}$

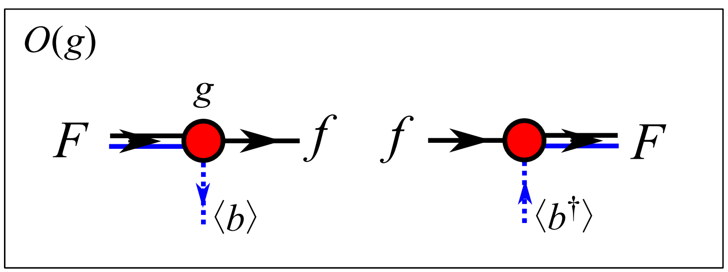

One-body mixing

$$V_{\mathrm{M}} = g\sqrt{\rho_b} \sum_{\boldsymbol{P}} (F_{\boldsymbol{P}}^{\dagger} f_{\boldsymbol{P}} + f_{\boldsymbol{P}}^{\dagger} F_{\boldsymbol{P}})$$

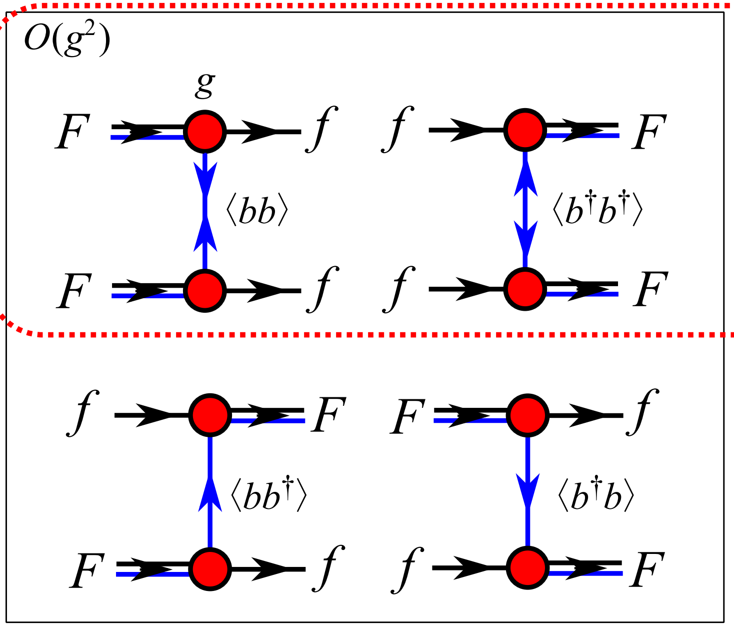

Pair-exchange coupling

Relevant to analog of pairing in QCD

$$V_{\mathrm{SMW}} = \frac{1}{2} \sum_{\boldsymbol{k},\boldsymbol{k}',\boldsymbol{P}} U_{\mathrm{SMW}}(\boldsymbol{q}, \omega) \times f_{\boldsymbol{k}+\boldsymbol{P}/2}^{\dagger} f_{-\boldsymbol{k}+\boldsymbol{P}/2}^{\dagger} F_{-\boldsymbol{k}'+\boldsymbol{P}/2} F_{\boldsymbol{k}'+\boldsymbol{P}/2} + \mathrm{H.c.},$$

Boson-exchange coupling

$$V_{\mathrm{PM}} = \frac{1}{2} \sum_{\boldsymbol{k},\boldsymbol{k}',\boldsymbol{P}} U_{\mathrm{PM}}(\boldsymbol{q}, \omega) \times F_{\boldsymbol{k}+\boldsymbol{P}/2}^{\dagger} F_{-\boldsymbol{k}'+\boldsymbol{P}/2} f_{-\boldsymbol{k}+\boldsymbol{P}/2}^{\dagger} f_{\boldsymbol{k}'+\boldsymbol{P}/2} + \mathrm{H.c.},$$

Ff pairing term (unfavored due to mass and population imbalances)

Mean-field theory of *P*-wave superfluid

Fermion-fermion interaction

$$V_{ff} = \frac{1}{2}\sum_{\boldsymbol{k},\boldsymbol{k}',\boldsymbol{q}} U_{ff}(\boldsymbol{k},\boldsymbol{k}') f^{\dagger}_{\boldsymbol{k}+\boldsymbol{q}/2} f^{\dagger}_{-\boldsymbol{k}+\boldsymbol{q}/2} f_{-\boldsymbol{k}'+\boldsymbol{q}/2} f_{\boldsymbol{k}'+\boldsymbol{q}/2}$$

Molecule-Molecule interaction

$$V_{FF} = \frac{1}{2}\sum_{\boldsymbol{k},\boldsymbol{k}',\boldsymbol{q}} U_{FF}(\boldsymbol{k},\boldsymbol{k}') F^{\dagger}_{\boldsymbol{k}+\boldsymbol{q}/2} F^{\dagger}_{-\boldsymbol{k}+\boldsymbol{q}/2} F_{-\boldsymbol{k}'+\boldsymbol{q}/2} F_{\boldsymbol{k}'+\boldsymbol{q}/2}$$

Suhl-Mattias-Walker*-type pair exchange

$$V_{\mathrm{SMW}} = \frac{1}{2}\sum_{\boldsymbol{k},\boldsymbol{k}',\boldsymbol{P}} U_{\mathrm{SMW}}(\boldsymbol{q},\omega) \times f^{\dagger}_{\boldsymbol{k}+\boldsymbol{P}/2} f^{\dagger}_{-\boldsymbol{k}+\boldsymbol{P}/2} F_{-\boldsymbol{k}'+\boldsymbol{P}/2} F_{\boldsymbol{k}'+\boldsymbol{P}/2} + \mathrm{H.c.},$$

*H. Suhl, B. T. Matthias, and L. R. Walker
Phys. Rev. Lett. **3**, 552 (1959).

Mean-field theory of *P*-wave superfluid

Fermion-fermion interaction

$$V_{ff} = \frac{1}{2}\sum_{\boldsymbol{k},\boldsymbol{k}',\boldsymbol{q}} U_{ff}(\boldsymbol{k},\boldsymbol{k}') f^{\dagger}_{\boldsymbol{k}+\boldsymbol{q}/2} f^{\dagger}_{-\boldsymbol{k}+\boldsymbol{q}/2} f_{-\boldsymbol{k}'+\boldsymbol{q}/2} f_{\boldsymbol{k}'+\boldsymbol{q}/2}$$

Molecule-Molecule interaction

$$V_{FF} = \frac{1}{2}\sum_{\boldsymbol{k},\boldsymbol{k}',\boldsymbol{q}} U_{FF}(\boldsymbol{k},\boldsymbol{k}') F^{\dagger}_{\boldsymbol{k}+\boldsymbol{q}/2} F^{\dagger}_{-\boldsymbol{k}+\boldsymbol{q}/2} F_{-\boldsymbol{k}'+\boldsymbol{q}/2} F_{\boldsymbol{k}'+\boldsymbol{q}/2}$$

Suhl-Mattias-Walker*-type pair exchange

$$V_{\mathrm{SMW}} = \frac{1}{2}\sum_{\boldsymbol{k},\boldsymbol{k}',\boldsymbol{P}} U_{\mathrm{SMW}}(\boldsymbol{q},\omega) \times f^{\dagger}_{\boldsymbol{k}+\boldsymbol{P}/2} f^{\dagger}_{-\boldsymbol{k}+\boldsymbol{P}/2} F_{-\boldsymbol{k}'+\boldsymbol{P}/2} F_{\boldsymbol{k}'+\boldsymbol{P}/2} + \mathrm{H.c.},$$

*H. Suhl, B. T. Matthias, and L. R. Walker Phys. Rev. Lett. **3**, 552 (1959).

P-wave pairing order parameter :Remaining global $U(1)_{f+F}$ is broken

$$\Delta_{ff}(\boldsymbol{k}) = -\sum_{\boldsymbol{k}'}[U^{*}_{\mathrm{SMW}}(\bar{q},\bar{\omega})\langle F_{-\boldsymbol{k}'}F_{\boldsymbol{k}'}\rangle + U_{ff}(\boldsymbol{k},\boldsymbol{k}')\langle f_{-\boldsymbol{k}'}f_{\boldsymbol{k}'}\rangle],$$

$$\Delta_{FF}(\boldsymbol{k}) = -\sum_{\boldsymbol{k}'}[U_{\mathrm{SMW}}(\bar{q},\bar{\omega})\langle f_{-\boldsymbol{k}'}f_{\boldsymbol{k}'}\rangle + U_{FF}(\boldsymbol{k},\boldsymbol{k}')\langle F_{-\boldsymbol{k}'}F_{\boldsymbol{k}'}\rangle].$$

Mean-field theory of *P*-wave superfluid

Fermion-fermion interaction

$$V_{ff} = \frac{1}{2}\sum_{\boldsymbol{k},\boldsymbol{k}',\boldsymbol{q}} U_{ff}(\boldsymbol{k},\boldsymbol{k}') f^{\dagger}_{\boldsymbol{k}+\boldsymbol{q}/2} f^{\dagger}_{-\boldsymbol{k}+\boldsymbol{q}/2} f_{-\boldsymbol{k}'+\boldsymbol{q}/2} f_{\boldsymbol{k}'+\boldsymbol{q}/2}$$

Molecule-Molecule interaction

$$V_{FF} = \frac{1}{2}\sum_{\boldsymbol{k},\boldsymbol{k}',\boldsymbol{q}} U_{FF}(\boldsymbol{k},\boldsymbol{k}') F^{\dagger}_{\boldsymbol{k}+\boldsymbol{q}/2} F^{\dagger}_{-\boldsymbol{k}+\boldsymbol{q}/2} F_{-\boldsymbol{k}'+\boldsymbol{q}/2} F_{\boldsymbol{k}'+\boldsymbol{q}/2}$$

Suhl-Mattias-Walker*-type pair exchange

$$V_{\mathrm{SMW}} = \frac{1}{2}\sum_{\boldsymbol{k},\boldsymbol{k}',\boldsymbol{P}} U_{\mathrm{SMW}}(\boldsymbol{q},\omega) \times f^{\dagger}_{\boldsymbol{k}+\boldsymbol{P}/2} f^{\dagger}_{-\boldsymbol{k}+\boldsymbol{P}/2} F_{-\boldsymbol{k}'+\boldsymbol{P}/2} F_{\boldsymbol{k}'+\boldsymbol{P}/2} + \mathrm{H.c.},$$

*H. Suhl, B. T. Matthias, and L. R. Walker Phys. Rev. Lett. **3**, 552 (1959).

P-wave pairing order parameter :Remaining global $U(1)_{f+F}$ is broken

$$\Delta_{ff}(\boldsymbol{k}) = -\sum_{\boldsymbol{k}'}[U^{*}_{\mathrm{SMW}}(\bar{q},\bar{\omega})\langle F_{-\boldsymbol{k}'}F_{\boldsymbol{k}'}\rangle + U_{ff}(\boldsymbol{k},\boldsymbol{k}')\langle f_{-\boldsymbol{k}'}f_{\boldsymbol{k}'}\rangle],$$

$$\Delta_{FF}(\boldsymbol{k}) = -\sum_{\boldsymbol{k}'}[U_{\mathrm{SMW}}(\bar{q},\bar{\omega})\langle f_{-\boldsymbol{k}'}f_{\boldsymbol{k}'}\rangle + U_{FF}(\boldsymbol{k},\boldsymbol{k}')\langle F_{-\boldsymbol{k}'}F_{\boldsymbol{k}'}\rangle].$$

$\langle FF\rangle \neq 0$ “**or**” $\langle ff\rangle \neq 0$ ⇒ “**Both**” $\Delta_{ff}(\boldsymbol{k}) \neq 0$ and $\Delta_{FF}(\boldsymbol{k}) \neq 0$

Supporting continuity

Suhl-Mattias-Walker-type pair-exchange interaction

Continuity can be understood via **two-band superconducting theory**

SMW interband pair-exchange coupling U_{12} in a two-band superconductor

$1 \rightarrow f, 2 \rightarrow F, U_{12} \rightarrow V_{\mathrm{SMW}}$

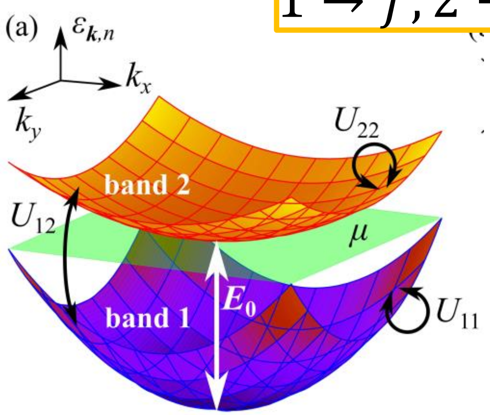

$|U_{22}| >> |U_{11}|$

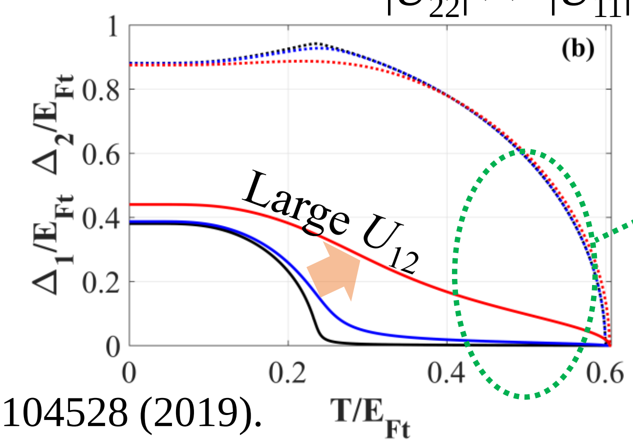

Both Δ_1 and Δ_2 become nonzero Below single T_c

Y. Yerin, HT, P. Pieri, and A. Perali, PRB **100**, 104528 (2019).

At $T = 0$

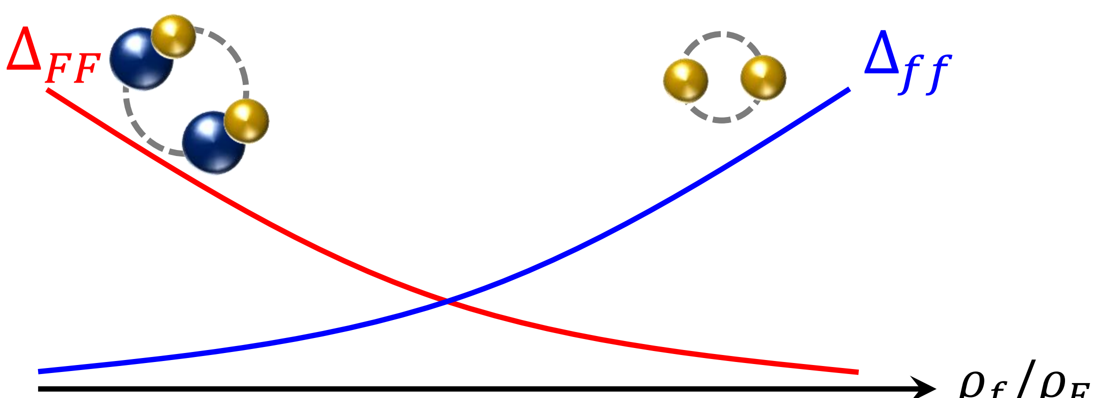

Infrared singularity

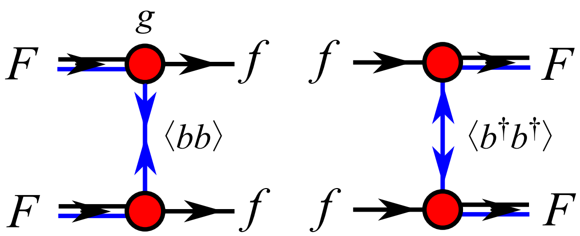

$$U_{\mathrm{SMW}}(\boldsymbol{q}, \omega) = g^2 D_{12}(\boldsymbol{q}, \omega)$$

<u>Anomalous propagator in Bogoliubov theory</u>

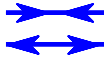

$$D_{12}(\boldsymbol{q}, \omega) = \frac{g_{bb}\rho_b}{(\omega - E_{\boldsymbol{q},b})(\omega + E_{\boldsymbol{q},b})}$$

<u>Superfluid phonon dispersion</u>

$$E_{\boldsymbol{q},b} = \sqrt{\frac{q^2}{2m_b}\left(\frac{q^2}{2m_b} + 2g_{bb}\rho_b\right)} \xrightarrow{\boldsymbol{q}\to 0} v_b q$$

$$\boxed{D_{12}(\boldsymbol{q}, \omega) \to \infty \text{ when } \omega = \pm E_{\boldsymbol{q},b} \sim \pm v_b q}$$

U_{SMW} diverges at low energies, no electrostatic screening…

Infrared singularity

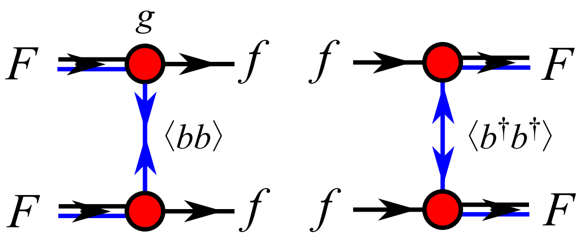

$$U_{\mathrm{SMW}}(\boldsymbol{q},\omega) = g^2 D_{12}(\boldsymbol{q},\omega)$$

Anomalous propagator in Bogoliubov theory

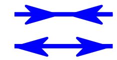

$$D_{12}(\boldsymbol{q},\omega) = \frac{g_{bb}\rho_b}{(\omega - E_{\boldsymbol{q},b})(\omega + E_{\boldsymbol{q},b})}$$

Superfluid phonon dispersion

$$E_{\boldsymbol{q},b} = \sqrt{\frac{q^2}{2m_b}\left(\frac{q^2}{2m_b} + 2g_{bb}\rho_b\right)} \xrightarrow{\boldsymbol{q}\to 0} v_b q$$

$$D_{12}(\boldsymbol{q},\omega) \to \infty \text{ when } \omega = \pm E_{\boldsymbol{q},b} \sim \pm v_b q$$

U_{SMW} diverges at low energies, no electrostatic screening…➡ **Dynamical screening**

Landau damping of phonon: $\Sigma_b =$

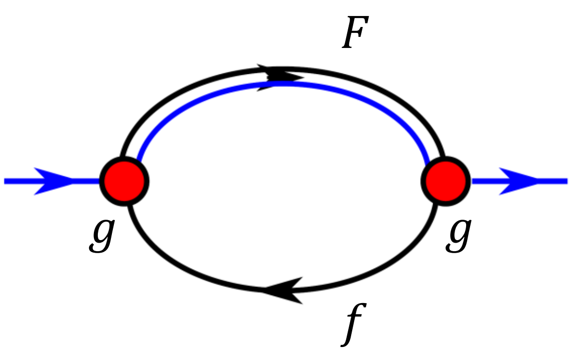

BCS-BCS crossover between molecular and atomic superfluid

Fermion EFT for stable and large BEC

$$E_{\text{Bose}} = -\mu_b \rho_b + \frac{1}{2} g_{bb} \rho_b^2$$

Density-dependent interaction

$$U_{\text{SMW}}(\boldsymbol{q}, \omega) \to U_{\text{SMW}}(|\boldsymbol{q}| = \bar{q}, \omega = \bar{\omega})$$

$$\bar{q} = \sqrt{k_f^2 + k_F^2 - 2k_f k_F \cos\theta_{\boldsymbol{kk}'}}, \quad \bar{\omega} = E_f - E_F$$

Fermi momentum and energy

$$k_i = (6\pi^2 \rho_i)^{1/3}, \quad E_i = \frac{k_i^2}{2m_i} \quad (i = f, F)$$

$$U_{\text{SMW}}(\bar{q}, \bar{\omega}) \simeq g^2 g_{bb} \rho_b e^{2i\theta_{\text{BEC}}} \frac{\alpha^2 \frac{\bar{\omega}^2}{\bar{q}^2} - v_b^2 \bar{q}^2}{\left(\alpha^2 \frac{\bar{\omega}^2}{\bar{q}^2} + v_b^2 \bar{q}^2\right)^2}$$

Infrared singularity is removed by the Landau damping

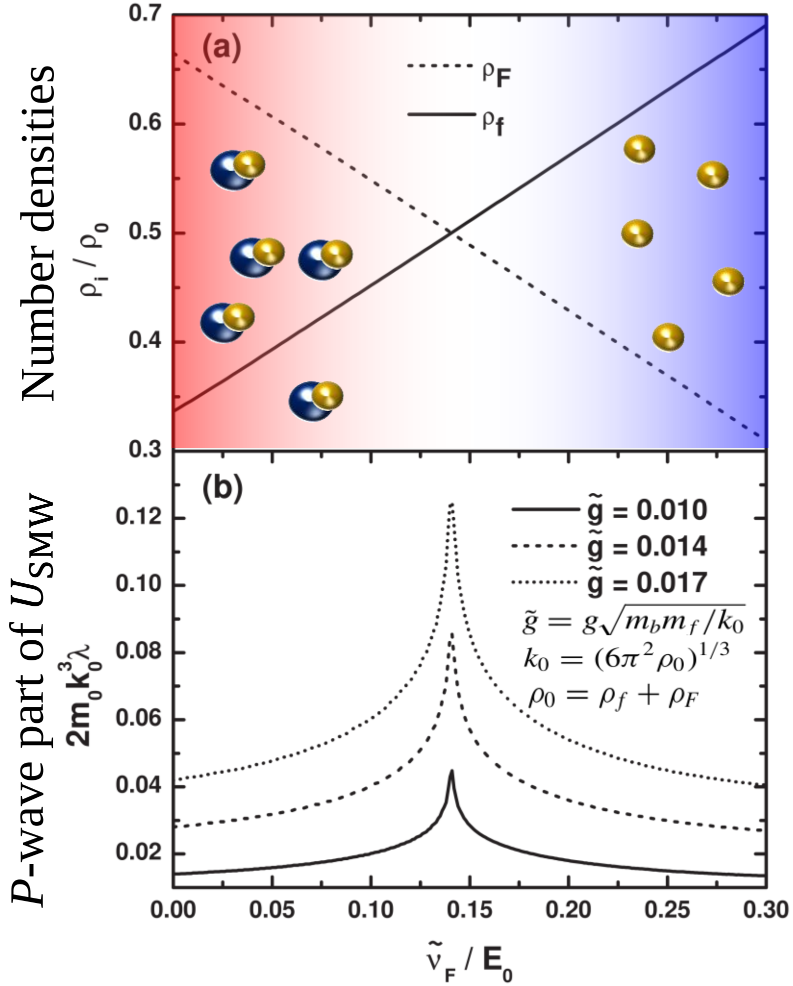

Molecular energy level
(experimentally tunable parameter)

BCS-BCS crossover between molecular and atomic superfluid

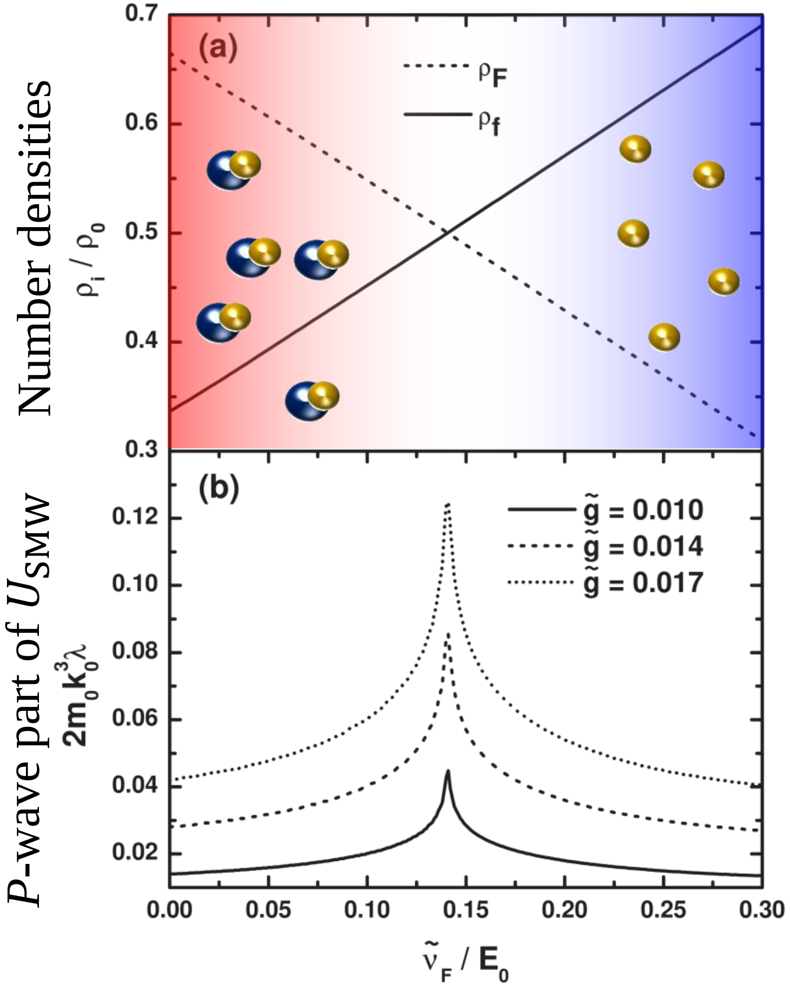

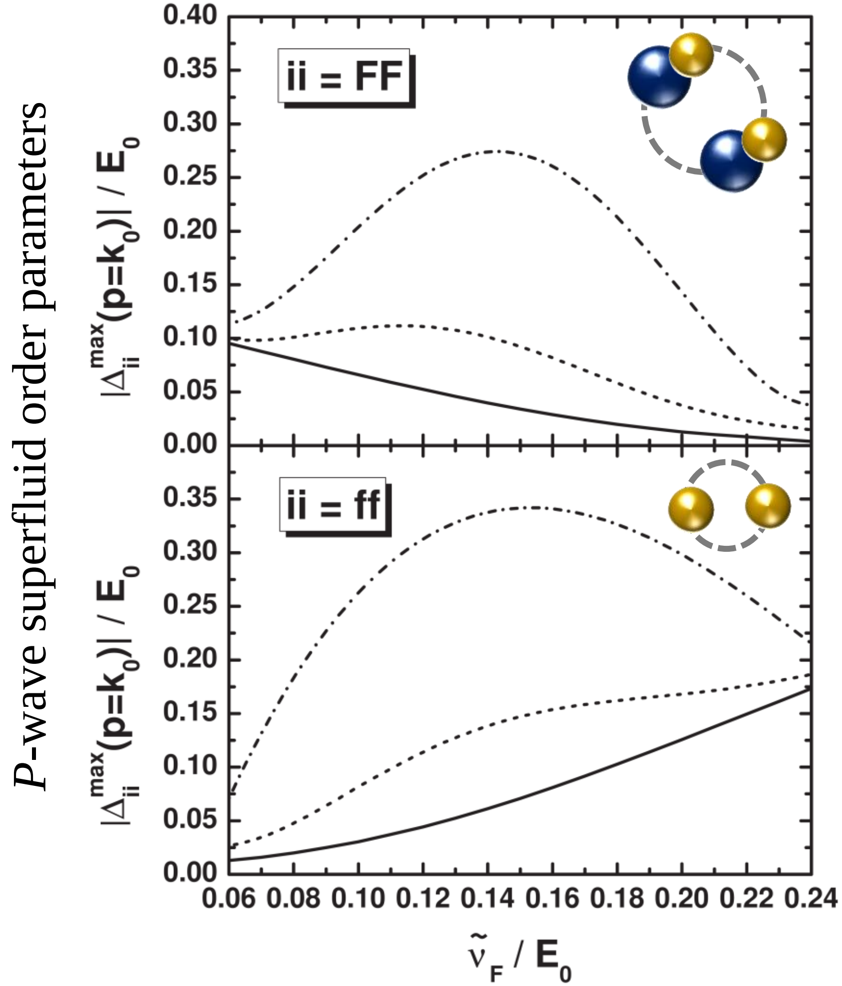

BCS-BCS crossover between molecular and atomic superfluid

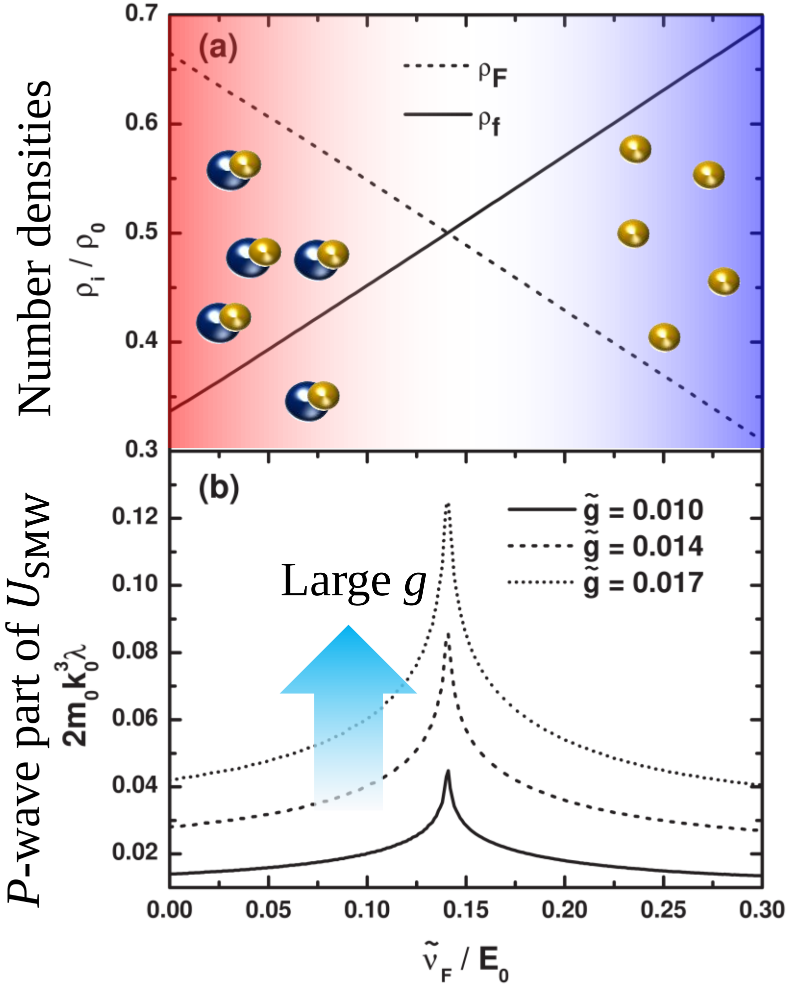

Molecular energy level

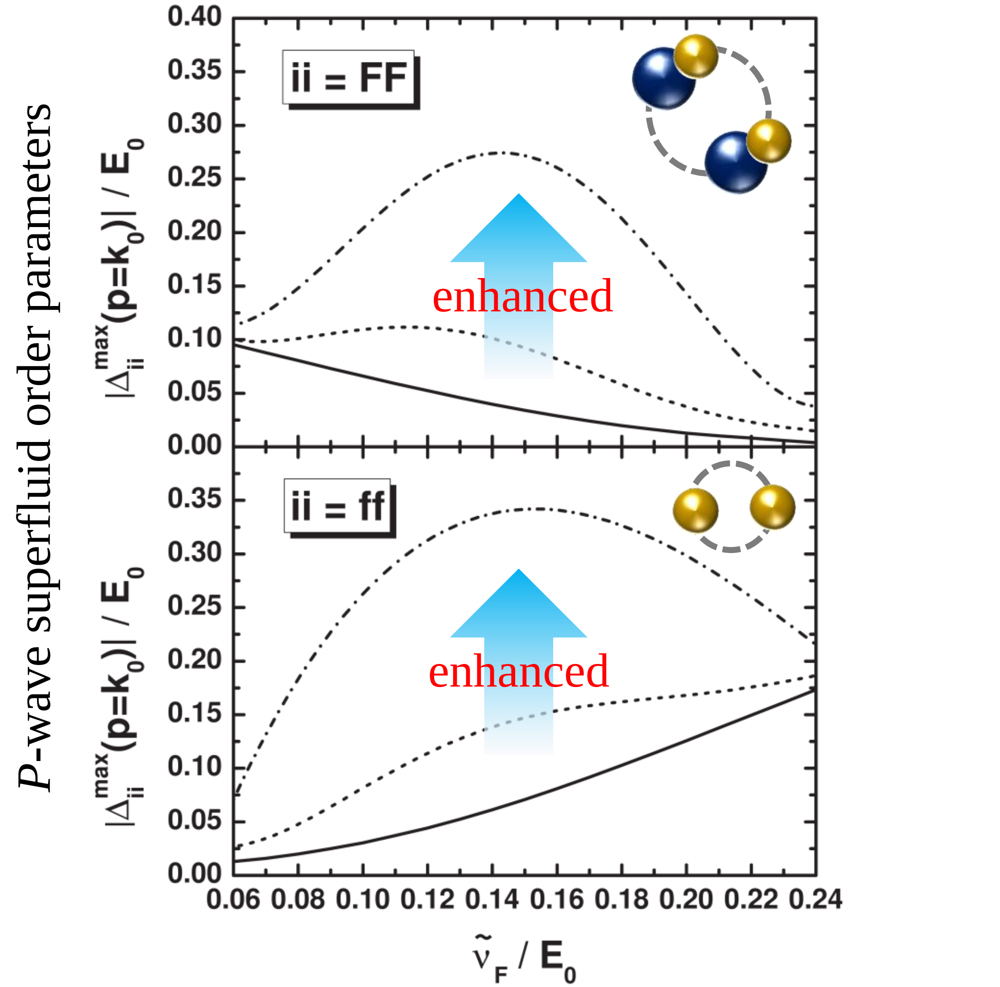

Molecular energy level

Outline

- Brief introduction of neutron superfluid
- $^3P_0$ neutron superfluid at low density
- Fate of P-wave pairing at high density
- Summary

Outline

- Brief introduction of neutron superfluid
- $^3P_0$ neutron superfluid at low density
- Fate of *P*-wave pairing at high density
- Summary

Summary

- We have explored a possibility of $^3P_0$ neutron superfluid, which has been overlooked because of several reasons regardless of a long history of nucleon-superfluid studies in neutron stars.
- $^3P_0$ neutron superfluid can appear at $T \lesssim 10^8$ K and $B \gtrsim 10^{17}$G. While it is still elusive if $^3P_0$ neutron superfluid can realize in nature or not, such a possibility for newly discovered astrophysical environments such as magnetars in the future.
- At high densities, we discuss the possible continuity between nucleon and quark P-wave superlfuids from the perspective of an ultracold Bose-Fermi mixture.
- The continuity between atomic and molecular P-wave superfluids in a Bose-Fermi mixture can be understood as an analog of a two-band superconductor with pair-exchange coupling. This might give a hint to understand the hadron-quark superfluid continuity.

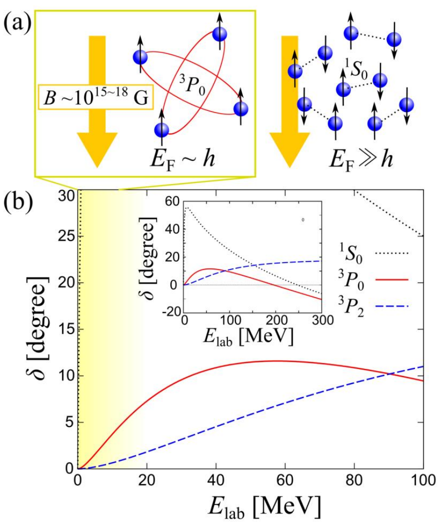

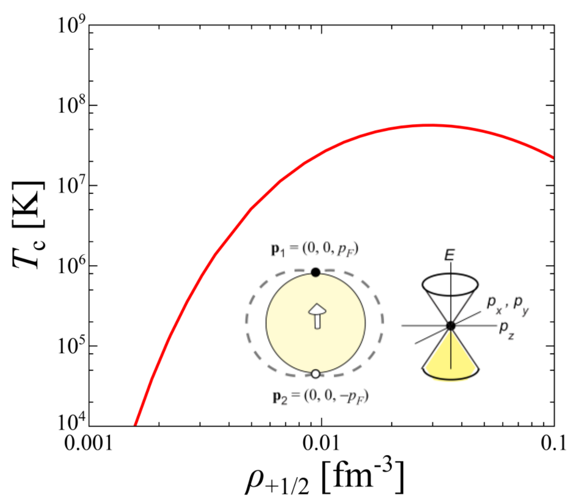

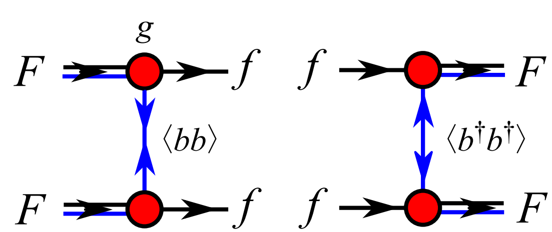

Future work: Competition of S- and P-waves, finite nuclei, backaction to BEC, strong coupling,…

Appendix

Competition between $^1S_0$ and $^3P_0$?

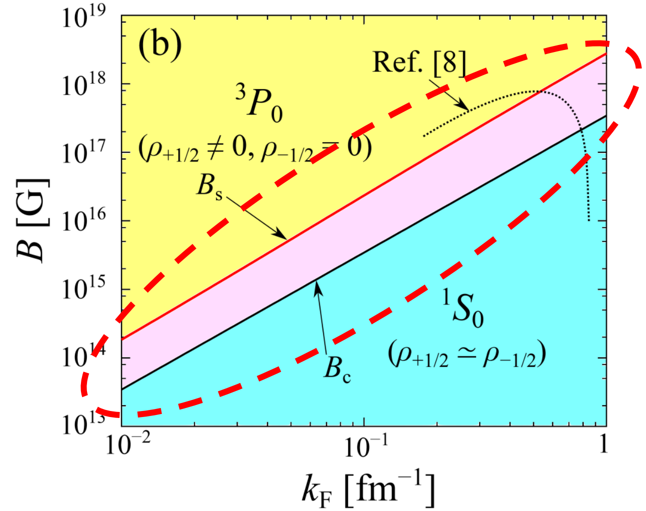

What happens in the region between $^3P_0$ and $^1S_0$ superfluids?

Low dim. in pasta

arXiv:1112.2018

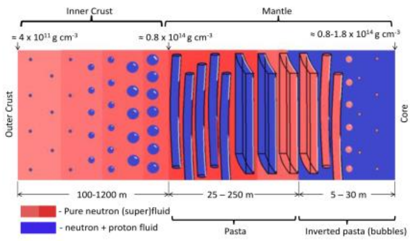

➡ Analogue system in cold atoms?

Overlapped S- and P-wave resonances

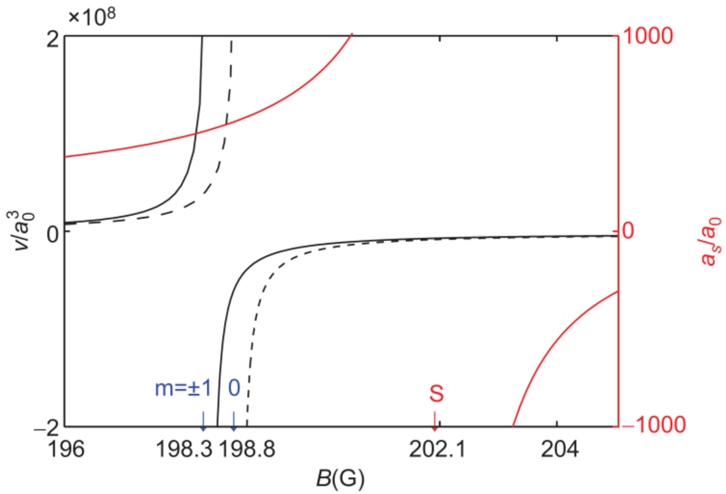

Sci. China Phys. Mech. Astron. **60**, 127011 (2017).

S- and P-wave interactions in q1D fermions

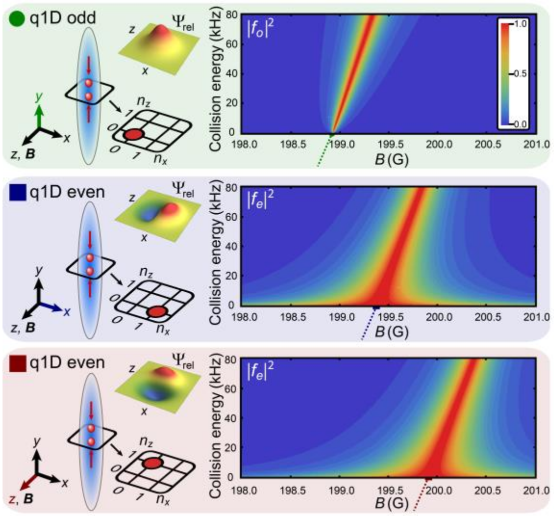

PRX **13**, 021013 (2023)

Pairing and tripling due to *S*- and *P*-wave interactions

Y. Guo and HT, Phys. Rev. B **107**, 024511 (2023).

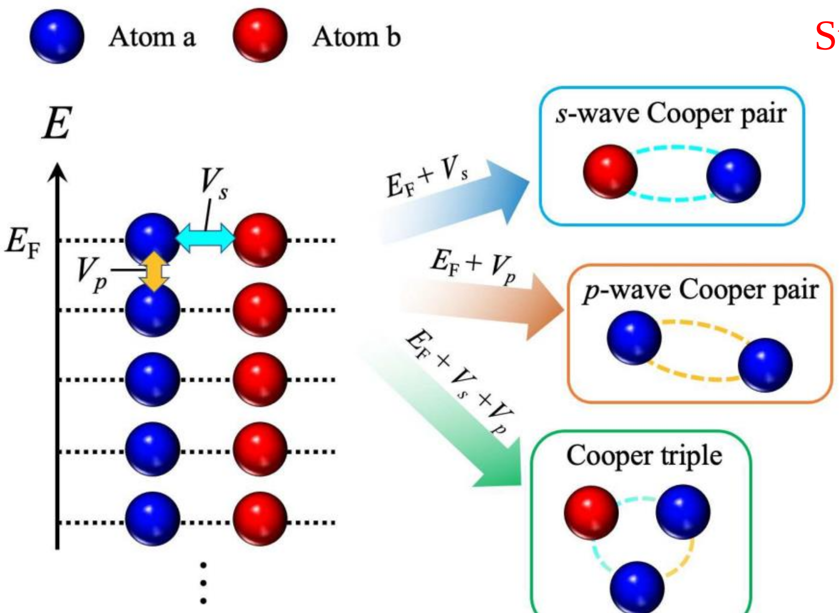

Phase diagram from the variational approach

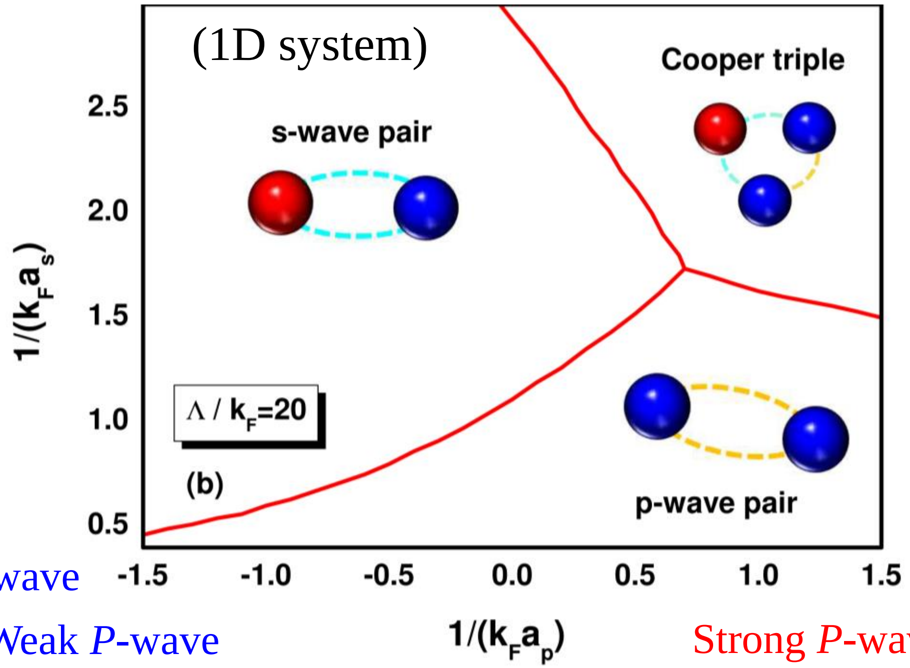

Landau damping effect on the pair-exchange interaction

$$U_{\rm SMW}(\boldsymbol{q},\omega) = g^2 D_{12}(\boldsymbol{q},\omega) = g^2 g_{bb}\rho_b e^{2i\theta_{\rm BEC}} \frac{\omega^2 - E_{\boldsymbol{q},b}^2 + \Gamma^2(\boldsymbol{q},\omega) - 2i\omega\Gamma(\boldsymbol{q},\omega)}{[(\omega - E_{\boldsymbol{q},b})^2 + \Gamma^2(\boldsymbol{q},\omega)][(\omega + E_{\boldsymbol{q},b})^2 + \Gamma^2(\boldsymbol{q},\omega)]}$$

Damping factor: $\Gamma(\boldsymbol{q},\omega) \equiv -{\rm Im}\Sigma_b(\boldsymbol{q},\omega) \simeq \frac{m_f m_F g^2}{4\pi^2}\frac{\omega}{q} \equiv \alpha\frac{\omega}{q}$

Density-dependent interaction at weak coupling

$$U_{\rm SMW}(\boldsymbol{q},\omega) \to U_{\rm SMW}(|\boldsymbol{q}| = \bar{q}, \omega = \bar{\omega})$$

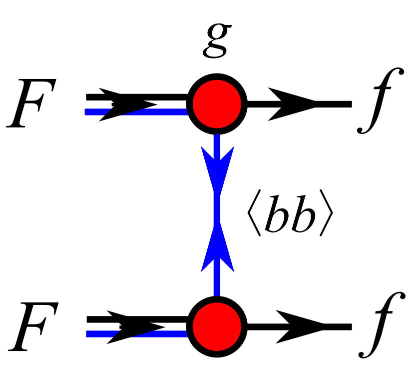

$$\bar{q} = \sqrt{k_f^2 + k_F^2 - 2k_f k_F \cos\theta_{\boldsymbol{kk}'}}, \quad \bar{\omega} = E_f - E_F$$

$$k_i = (6\pi^2\rho_i)^{1/3}, \quad E_i = \frac{k_i^2}{2m_i} \quad (i = f, F)$$

$$U_{\rm SMW}(\bar{q},\bar{\omega}) \simeq g^2 g_{bb}\rho_b e^{2i\theta_{\rm BEC}} \frac{\alpha^2\frac{\bar{\omega}^2}{\bar{q}^2} - v_b^2\bar{q}^2}{\left(\alpha^2\frac{\bar{\omega}^2}{\bar{q}^2} + v_b^2\bar{q}^2\right)^2}$$

Relation to two-band superconductor

Hadron-quark continuity $\simeq$ Atomic-molecule continuity $\simeq$ Two-band superconductor

<u>Dispersive and heavy bands</u>

$$H = \sum_{i,\boldsymbol{k},\sigma} \xi_i(\boldsymbol{k}) c^\dagger_{\boldsymbol{k},\sigma,i} c_{\boldsymbol{k},\sigma,i} + \sum_{i,j} \sum_{\boldsymbol{k},\boldsymbol{k}'} V_{ij}(\boldsymbol{k},\boldsymbol{k}') B^\dagger_{\boldsymbol{k},i} B_{\boldsymbol{k}',j}$$

Pair operator: $B_{\boldsymbol{k},j} = c_{-\boldsymbol{k},\downarrow,j} c_{\boldsymbol{k},\uparrow,j}$,

$j = 1{,}2$: band index

K. Ochi, HT, K. Iida, and H. Aoki, PRR **4**, 013032 (2022)

<u>Atomic and molecular superfluid</u>

$$H_{\text{eff}} \simeq \sum_{\boldsymbol{p}} \varepsilon_{\boldsymbol{p},f} f^\dagger_{\boldsymbol{p}} f_{\boldsymbol{p}} + \sum_{\boldsymbol{p}} \varepsilon_{\boldsymbol{p},F} F^\dagger_{\boldsymbol{p}} F_{\boldsymbol{p}} + E_{\text{BEC}}$$

$$+ \frac{1}{2} \sum_{\boldsymbol{k},\boldsymbol{k}',\boldsymbol{P}} U_{\text{SMW}}(\boldsymbol{q},\omega) f^\dagger_{\boldsymbol{k}+\boldsymbol{P}/2} f^\dagger_{-\boldsymbol{k}+\boldsymbol{P}/2} F_{-\boldsymbol{k}'+\boldsymbol{P}/2} F_{\boldsymbol{k}'+\boldsymbol{P}/2} + \text{H.c.}$$

f: Fermi atom op. F: Fermi molecule op.

Y. Guo, HT, T. Hatsuda, and H. Liang, PRA **108**, 023304 (2023).

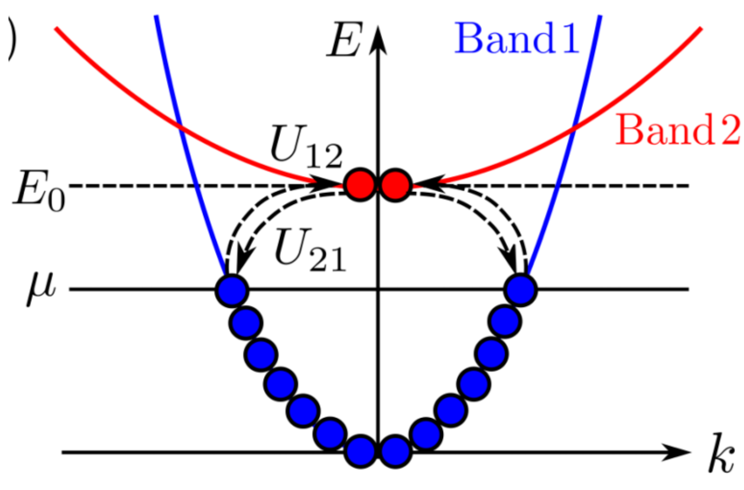

<u>Dispersive band 1</u>

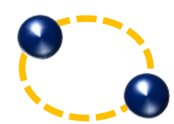

<u>Heavy band 2</u>
(band offset E_0)

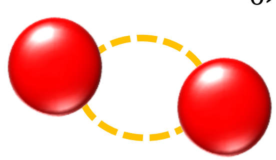

<u>Fermi atoms</u>

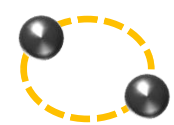

<u>Fermi molecules</u>
(Feshbach level E_0)

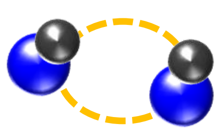

Spin polarization in the Skyrme interaction model

A. A. Isaev and J. Yang, Phys. Rev. C **80**, 065801 (2009).

<u>Spin polarization</u>

$$\Pi = \frac{\varrho_\uparrow - \varrho_\downarrow}{\varrho}$$

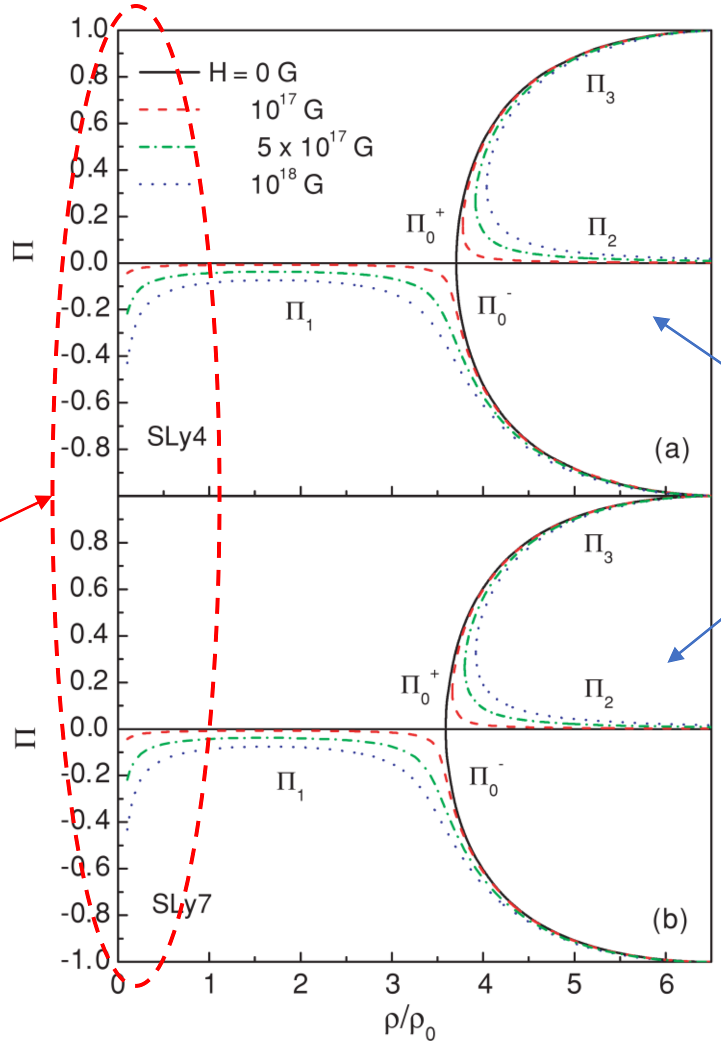

Overlooked!

Itinerant ferromagnetism (Stoner-type) at very high density ($\rho \gtrsim 3.8\rho_0$)

Is it possible to study spin polarization of dilute matter in more definite way?

➡ low-energy universality with cold atoms